S-CUBED
A Division of Maxwell Laboratories, Inc.

W/O 31171

SSS-TR-91-12742
DRAFT

ANALYSIS OF PRELIMINARY TESTING OF WILLIS HULIN WELL NO. 1

T. D. Riney

Technical Report

Work Performed for
U. S. Department of Energy
Geothermal Division

Under Subcontract to
Lawrence Berkeley Laboratory
DOE/LBL Contract No. DE-AC03-76SF00098

September 1991

P.O. Box 1620, La Jolla, California, 92038-1620
(619) 453-0060

DISCLAIMER

TABLE OF CONTENTS

LIST OF FIGURES

Figure **Page**

Figure **Page**

LIST OF TABLES

1. INTRODUCTION

The U. S. Department of Energy (DOE) has both drilled and tested four deep research wells in the Texas-Louisiana Gulf Coast region as part of its program to define the magnitude and recoverability of the geopressured-geothermal energy resource. DOE also took over nine wells from industry (before being abandoned) and tested them for short periods to determine fluid properties. The Willis Hulin Well No. 1, located about 7.5 miles south of the town of Erath, Louisiana, is the first well taken over from industry for possible long-term testing. This well penetrates the deepest known Gulf Coast geopressured-geothermal reservoir.

Prior to DOE accepting the Hulin well from Superior Oil Company in 1984, regional geologic work, by the Louisiana Geological Survey, Louisiana State University (LSU), had indicated that a massive sandstone about 500 feet thick at a depth of ~ 20,200 feet in the Hulin area (eastern quarter of the larger Bayou Herbert prospect) offered the most potential for geopressured-geothermal resource development (Bebout, *et al.*, 1982). The Bureau of Economic Geology, University of Texas at Austin, (UTA), subsequently compiled the available data for the Hulin area and conducted a geological investigation of the sandstone at 20,200 feet (Hamlin and Tyler, 1988). Only the Hulin well penetrated the target sandstone; insufficient data exist for determining the precise depositional setting. Hamlin and Tyler (1988) suggest the target sandstone represents a slope canyon fill or a dip-elongated submarine fan deposit. The thin mudstones (or shale) interbeds that vertically compartmentalize the main reservoir sandstone are thin and vertical flow communication across them may be affected by faulting.

Recently, LSU (see John, 1991) reanalyzed available seismic data and developed the seismic structure map shown in Figure 1. The top of the geologic structure is reported to be located near the Hulin well and the nearest mapped major boundary growth fault is over 3,000 feet from the well. Smaller internal faults are suspected but could not be located from the available information.

British Gas Exploration apparently has a different geologic interpretation than the LSU model. It is currently drilling a gas well into the same sand/shale sequence targeted by DOE at the Hulin well. The new well is about a mile northeast of the Hulin well; the site is outside the area considered by LSU to be the top of the structure. If drilling and flow test data from this well become available it may be possible to resolve the differences in geologic interpretation. Inter-well interference data would also help locate unmapped internal flow boundaries.

Analysis of the preliminary flow testing of the Hulin well during November 1989–January 1990 is presented in this report. The near-well permeability of the tested formation (~ 15–25 md) is considerably smaller than the near-well permeabilities at DOE's Gladys McCall (~ 85–133 md) and Pleasant Bayou (~ 200 md) design wells. The limited Hulin

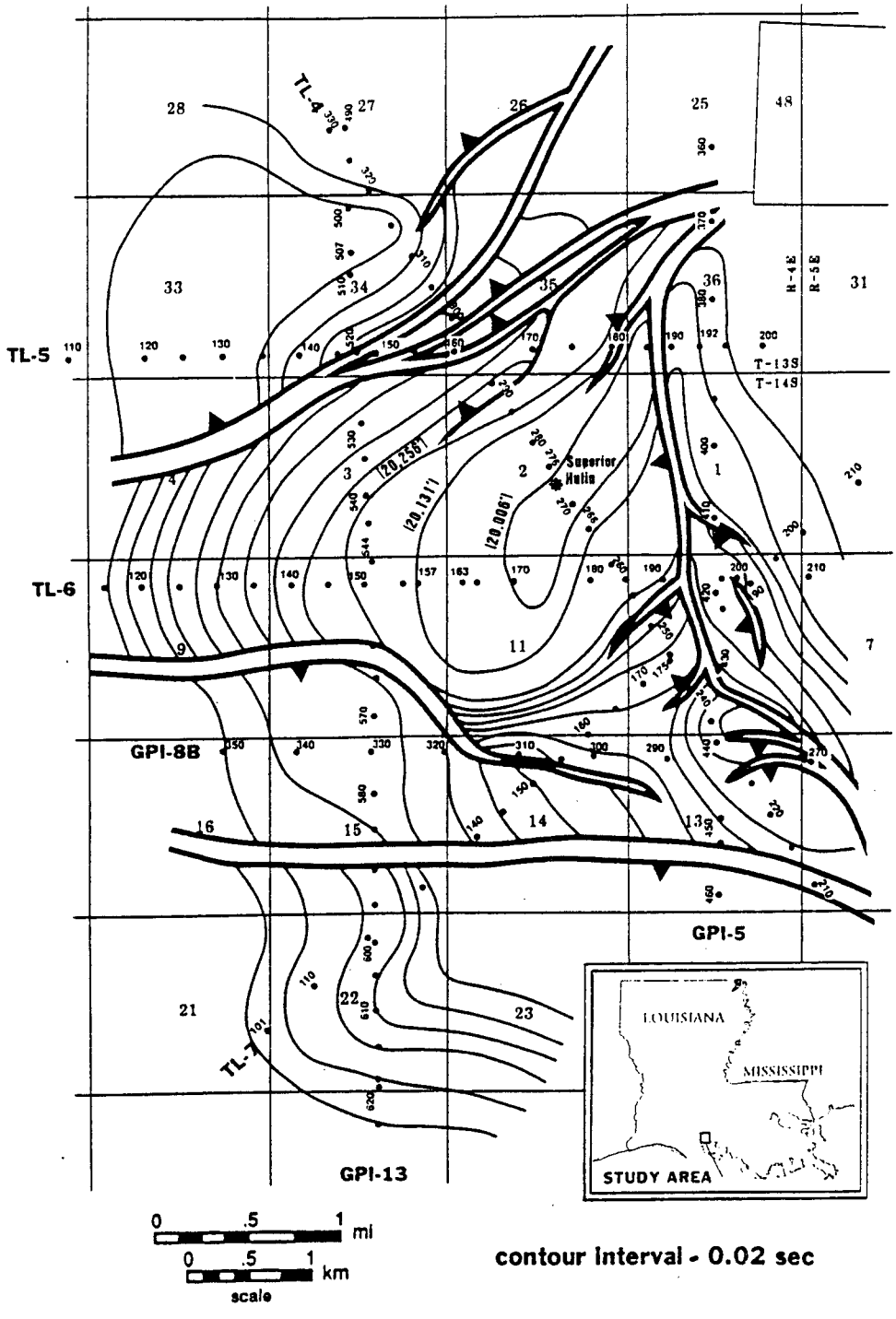

Figure 1. **Seismic structure map of Hulin geopressured-geothermal resource (prepared by LSU). Seismic wave travel time data from indicated stations used to map top of structure depth and major growth fault locations.**

production data imply that the proximal connected pore volume of the target sand-shale sequence (20,220–20,690 feet) is only about 180 million barrels. The nearest hydraulic barrier is ~ 90–130 feet from the Hulin well, and a second barrier appears to be present at a distance much closer to the well than the mapped growth faults (Figure 1). A simple rectangular reservoir configuration with a pore volume of 180 million barrels is used to represent the proximal reservoir and to provide a match to the pressure history data recorded during the preliminary testing.

The LSU seismic structure map indicates fault closure on the north, south and east but not on the west side. John (1991) notes that the areal extent of the target reservoir sand/shale sequence is undetermined, and details about lateral and vertical stratigraphic relationships and fluid communications between neighboring sands remain unknown. The LSU reservoir pore volume estimate of approximately 1 billion barrels is considered conservative. Based on experience from long-term testing at the Gladys McCall and Pleasant Bayou sites, we suspect that remote (poorly connected) reservoir volume at Hulin might also provide pressure support during long-term production testing.

2. WELL HISTORY

Willis Hulin Well No. 1 was spudded by Superior Oil Company in April 1978 as an exploration well, with a proposed depth of 21,000 feet. After reaching that depth without finding pay, a decision was made to drill deeper. While deepening, the drill pipe became stuck at 20,200 feet, and the hole was sidetracked to a depth of 21,546 feet. The well was completed and produced from the interval 21,059–21,094 feet by Superior Oil Company. The well produced about 0.3 BCF of gas and the surface tubing pressure declined from about 8,000 to 1,000 psia in nineteen months. At that point the well loaded up with liquid; apparently, a packer or tubing/casing failure had occurred.

Superior Oil Company turned the Hulin well over to DOE during 1984 for evaluation under its Geopressured Geothermal Program. The well penetrates a large geopressured region below ~ 12,500 feet and a thick sand/shale sequence in the Planulina zone was targeted by DOE for testing. The target sequence extends from about 20,220 feet to 20,690 feet and is overlain/underlain by thick shales. The total sequence thickness of ~ 470 feet may be considered to be comprised of six sand packages separated at the wellbore by five thin shale layers as shown in Table 1.

Table 1. Sand/shale layer thicknesses at sandface of Willis Hulin Well No. 1.

Sand No.	Sand Package	Shale Layer
6	20,220–20,352	20,352–20,358
5	20,358–20,385	20,385–20,393
4	20,393–20,437	20,437–20,448
3	20,448–20,548	20,548–20,558
2	20,558–20,600	20,600–20,616
1	20,616–20,690	

During the period from November 1988 to February 1989 Eaton Operating Company (EOC) cleaned out and reworked the Hulin well for preliminary testing (Eaton, *et al.*, 1990). During recompletion, the well was plugged back to 20,725 feet and the bottom 20 feet of the deepest sand package was perforated using a gun small enough to pass through the surface plumbing (less than 2 inches in diameter) and the 3.5-inch tubing above the depth of 15,988

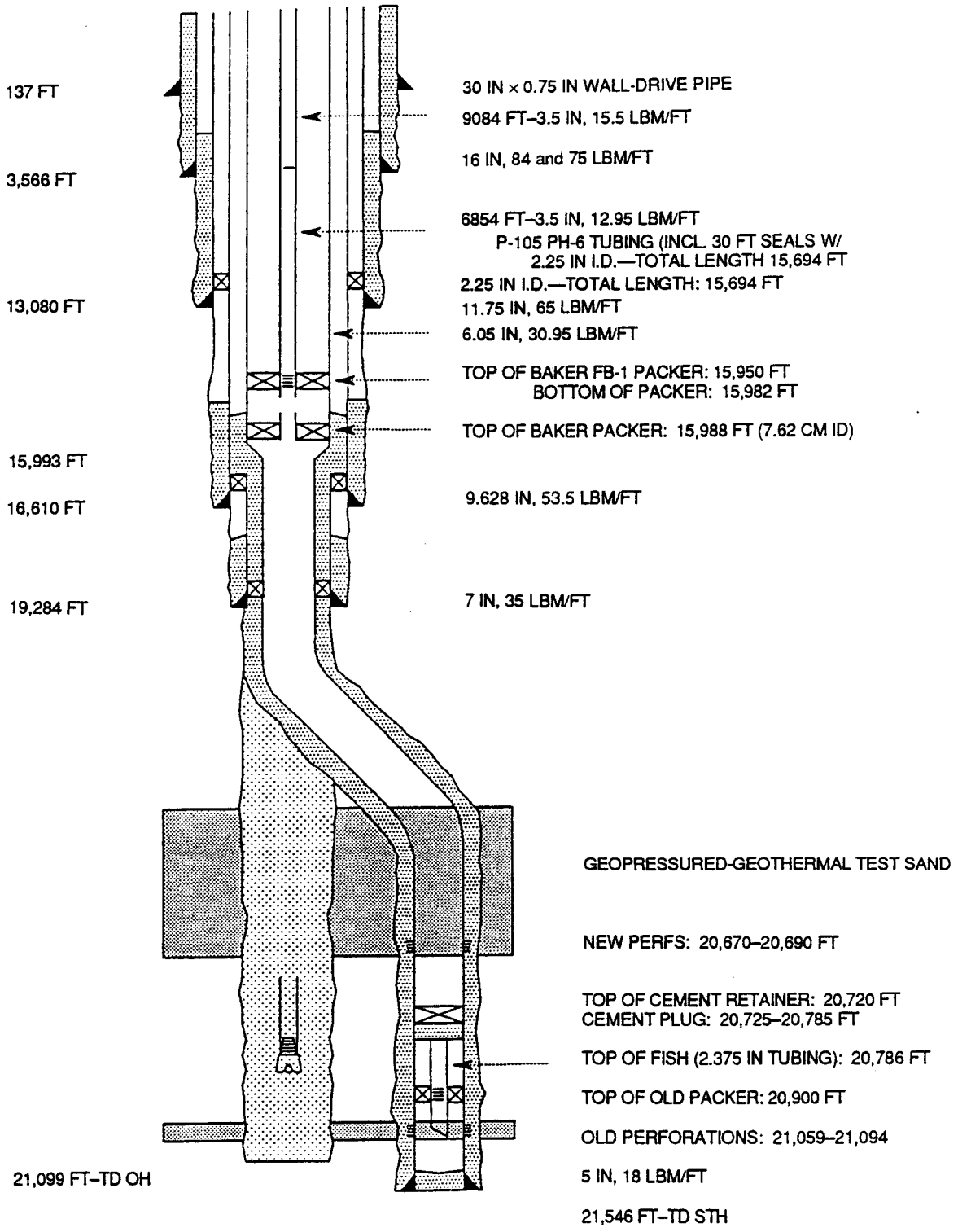

Figure 2. Willis Hulin Well No. 1 schematic as recompleted by EOC (February 08, 1989).

feet (Figure 2). After perforating 20,670 to 20,690 feet, the well was shutin because of DOE budget constraints. During DOE's 1990 Fiscal Year, EOC drilled an injection well for disposing of the waste brine. The deep test well was then reentered and preliminary flow tests performed (November 1989–January 1990). Analysis of these short flow tests will be presented here using the approximations given in Table 2 for the measured flow rates. We have relied heavily on the production reports prepared by the Institute of Gas Technology (Randolph and Rogers, 1989–1990) for the basic data used in the analysis. Note that well cleanup flow periods (in February and November, 1989) prior to the start of Flow Test No. 1 are not included in Table 2.

Table 2. Willis Hulin Well No. 1 flow rates during 1989–90 Preliminary Test.

Test Day	Date	Time	Elapsed Time (Hours)	Cumulative, Q (barrels)	Rate, q (bbl/day)
Flow Test No. 1					
1	12-06-89	16:49:20	0.	0.	2,423.
3	12-08	05:03:10	36.2306	3,658.	0.
5	12-10	19:00:00	98.1778	3,658.	2,407.
6	12-11	05:00:00	108.1778	4,661.	0.
	12-12,13	[additional perforations in deepest sand package]			
8	12-13	10:30:00	161.6778	4,661.	2,573.
9	12-14	05:20:00	180.5111	6,680.	0.
Flow Test No. 2					
12	12-17	17:04:16	264.2489	6,680.	2,027.
13	12-18	05:00:35	276.1875	7,688.	3,760.
17	12-22	03:47:19	370.9663	22,537.	0.
Flow Test No. 3					
	01-03	[shallowest sand package perforated]			
30	01-04-90	09:00:00	688.1778	22,537.	3,445.
32	01-06	18:36:00	745.7778	30,805.	2,440.
33	01-07	15:00:00	766.1778	32,879.	3,812.
34	01-08	15:00:00	790.1778	36,691.	0.
35	01-09	09:23:00	808.5611	36,691.	1,910.
37	01-11	05:00:00	852.1778	40,163.	0.

3. PRELIMINARY FLOW TESTING

On November 20, 1989, a P/T log was run in the shutin Hulin test well to determine stable pressure/temperature gradients prior to flow testing the well. At 20,600 feet the values recorded were 17,308 psia and 337.9°F (Table 3). The top of geopressure is located approximately at the base of the main series of Miocene sands, and the base is at about 12,500 feet in the Hulin well. A linear approximation to the full set of stable temperature data available below the top of the geopressured zone extrapolates to a value of ~ 342°F at 20,600 feet (Figures 3a and 3b). When the well was later flowed from the perforated interval (20,670–20,690 feet), the measured fluid temperatures reached 341.8°F, in good agreement with the temperature gradient extrapolation. Consequently, the stable pressure and temperature values at 20,600 feet are estimated to be

0.84 psia/ft

$$P_0 = 17{,}308 \text{ psia} \qquad T_0 = 342°\text{F}.$$

Table 3. Stable P/T measurements in Willis Hulin Well No. 1 (Nov. 20, 1989).

Depth (feet)	Pressure (psia)	Temperature (°F)
26	7,632	61.5
500	7,841	70.7
1,000	8,035	76.1
1,500	8,219	81.7
2,000	8,439	86.4
15,000	14,653	263.1
17,000	15,590	291.6
18,000	16,060	306.6
19,000	16,519	321.0
20,000	17,013	333.5
20,600	17,308	337.9

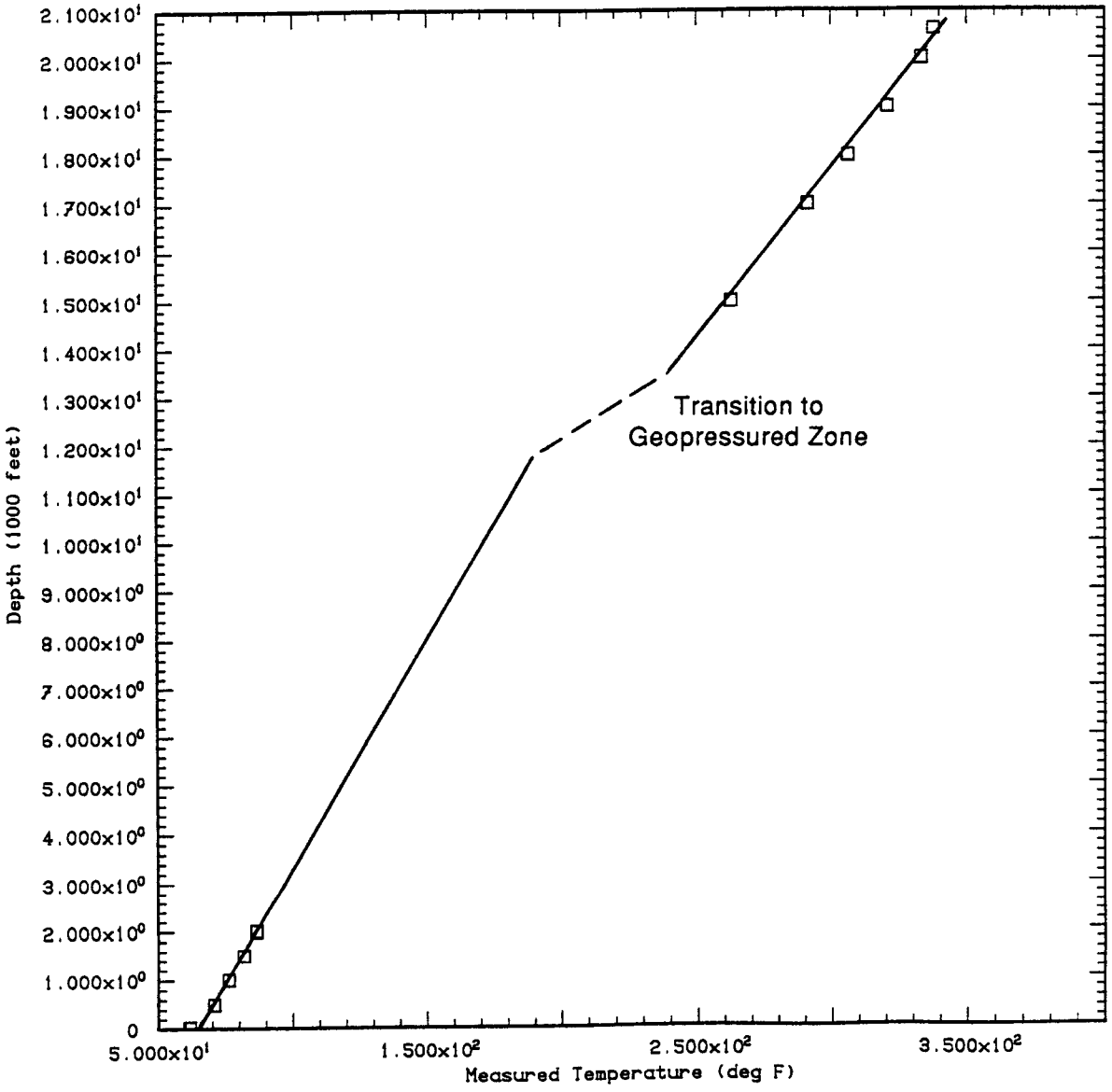

Figure 3a. Stable temperature gradient data measured during P/T logging of Willis Hulin Well No. 1 on November 20, 1989. Complete profile showing transition from hydrostatic to geopressured zone.

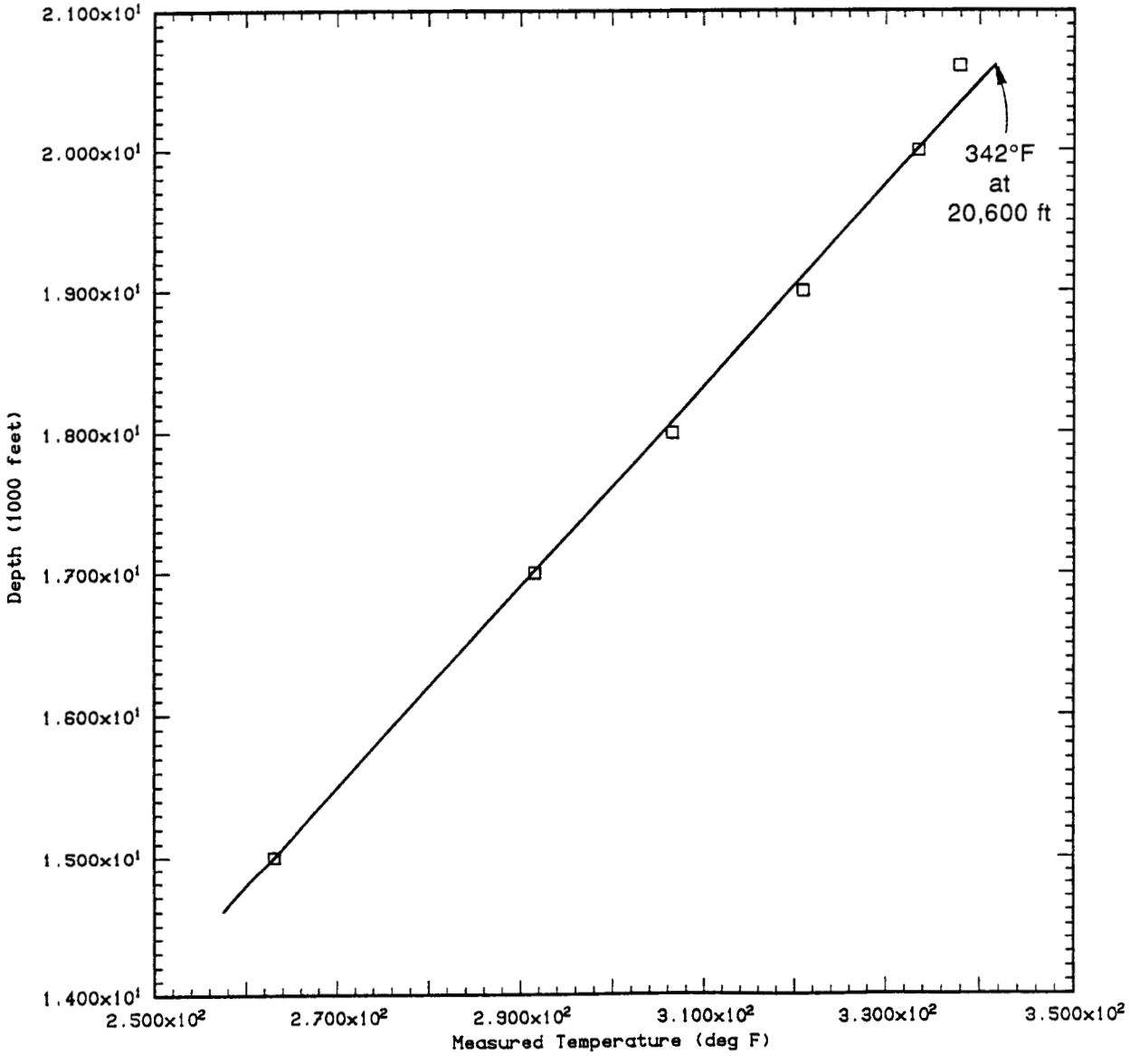

Figure 3b. Stable temperature gradient data measured during P/T logging of Willis Hulin Well No. 1 on November 20, 1989. Temperature gradient below the top of the geopressured zone.

On November 21, 1989, approximately 1,000 bbl of brine were produced during well cleanup flow. The well was then shutin for pressure recovery prior to starting Flow Test No. 1.

3.1 FLOW TEST NO. 1

The deepest sand package of thickness h = 74 feet (20,616–20,690 feet) was selected for initial testing. The bottom 20 feet of this package had been perforated by EOC (i.e. 20,670–20,690 feet) in February, 1989 after recompleting the well (Figure 2). The extent to which the small charges penetrated into the formation beyond the 7-inch casing is unknown.

A Panex P/T gauge was lowered to 20,600 feet in the cleaned out, shutin well on December 05, 1989 and allowed to stabilize overnight. The stable pressure and temperature values recorded at 20,600 feet were

$$P_1 = 17{,}294 \text{ psia} \qquad T_1 = 338.2°\text{F}.$$

The well was opened to flow at 16:49:20 on December 06 and flowed at an average rate of 2,423 b/d until shutin at 05:03:10 on December 08, 1989. The bottomhole pressure and temperature at 20,600 feet were recorded by Milton L. Cooke during the ~ 36 hours of drawdown and for ~ 52 hours of buildup subsequent to shutin. At the time of shutin the flowing pressure and temperature values recorded at 20,600 feet were

$$P_{wf} = 14{,}783 \text{ psia} \qquad T_{wf} = 341.0 \text{ F}.$$

Prior to opening the well on December 06 and again prior to shutting the well on December 08, EOC briefly lowered the Panex gauge on the wireline to check bottom depth. In both instances, the tool would not go below 20,675 feet which might indicate that as little as 5 feet of the perforated interval (20,670–20,690 feet) were open. In each case the gauge was returned to 20,600 feet after the brief period required to check the bottom depth.

Figure 4 presents a cartesian plot of the recorded bottomhole pressures (at 20,600 feet) during both the drawdown and buildup phases of Flow Test No. 1. Injection of about ten gallons of diesel oil into the wellbore corrupts a portion of the pressure buildup data. The diesel oil was pumped into the wellbore to displace the top of the brine to prevent formation of solid hydrates from compounds of methane and water. Details of the analysis leading to this procedure are summarized in an IGT report (Randolph and Rogers, 1989).

3.2 FLOW TEST NO. 2

On December 12, 1989 EOC perforated the intervals from 20,646 to 20,666 feet (first shot) and from 20,622 to 20,642 feet (second shot); on December 13 the interval 20,602 to

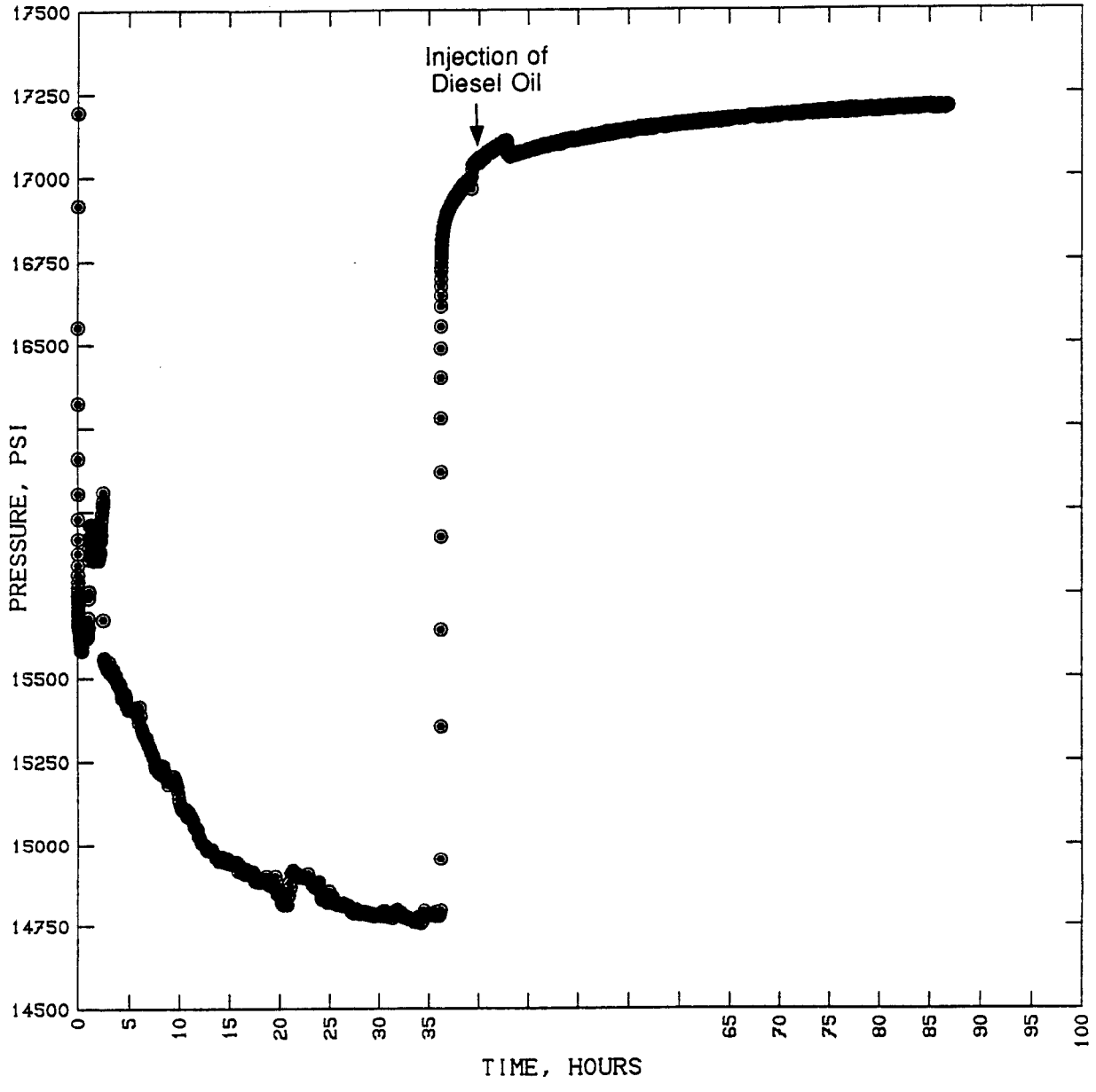

Figure 4. **Bottomhole pressure transient data from Flow Test No. 1. Gauge at 20,600 feet depth.**

20,642 feet was perforated. The well was flowed, from the newly perforated interval (20,602–20,666 feet) and the originally perforated interval (20,670–20,690 feet), on December 13–14 to clean out the well.

The Panex P/T gauge was recalibrated and on December 17, 1989 it was lowered in the shutin well to a maximum depth of 20,600 feet; it was then pulled back to 20,525 feet to raise the bottom of the sinker bars to above the shallowest perforation (20,602 feet). The well remained shut and allowed to stabilize for about fourteen hours. The pressure and temperature measured at 20,525 feet, after the well had been shut for about 83.7 hours, were

$$P_2 = 17{,}157 \text{ psia} \qquad T_2 = 336.5 \text{ F.}$$

The well was opened to flow at 17:04:16 on December 17, 1989. The bottomhole pressure and temperature (at 20,525 feet) were continuously recorded by Milton L. Cooke during the ~ 131 hours of drawdown and during the first ~ 99 hours of pressure buildup subsequent to shutin. At the time of shutin the flowing pressure and temperature values recorded at 20,525 feet were

$$P_{wf} = 14{,}458 \text{ psia} \qquad T_{wf} = 338.4 \text{ F.}$$

On January 2, 1990 a trip was made in and out of the well with the Panex gauge to record late-time buildup pressures and temperatures. Measurements were made until the gauge had stablized at the datum level (20,525 feet). The P/T values recorded at 13:00:26 on January 2 (Elapsed Time = 644.1850 hours, i.e. 379.94 hours after shutin) were 17,090 psia and 334.5°F.

Figure 5 presents a linear plot of the recorded bottomhole pressures (at 20,525 feet) during both the drawdown and buildup phases of Flow Test No. 2. The pressures recorded on December 17 (December 27) while lowering (raising)the gauge are not included in this plot. The pressure measured at 20,525 feet on January 2, 1990, after the well had been shut for about 380 hours, is also shown in Figure 5.

3.3 FLOW TEST NO. 3

On January 3, 1990 EOC sequentially fired two perforating guns in the interval 20,220–20,260 feet at the top of the shallowest sand package in the target sand/shale sequence. When each gun was fired there was an immediate increase of about 20 psi in the wellhead pressure. The overall change in wellhead pressure between 06:00 (before rigging up to perforate) and 23:00 (after rigging down the perforating gear) on January 3 was from 7,482 to 7,590 psia. This indicates that reservoir fluid pressures at 20,220–20,260 feet are much higher than the pressures in the wellbore at these levels prior to perforating. Presumably, the shallower perforations triggered the onset of internal flow through the wellbore, from the shallower horizon (20,220–20,260 feet) into the deeper horizon (i.e., 20,602–20,690 feet) that had been

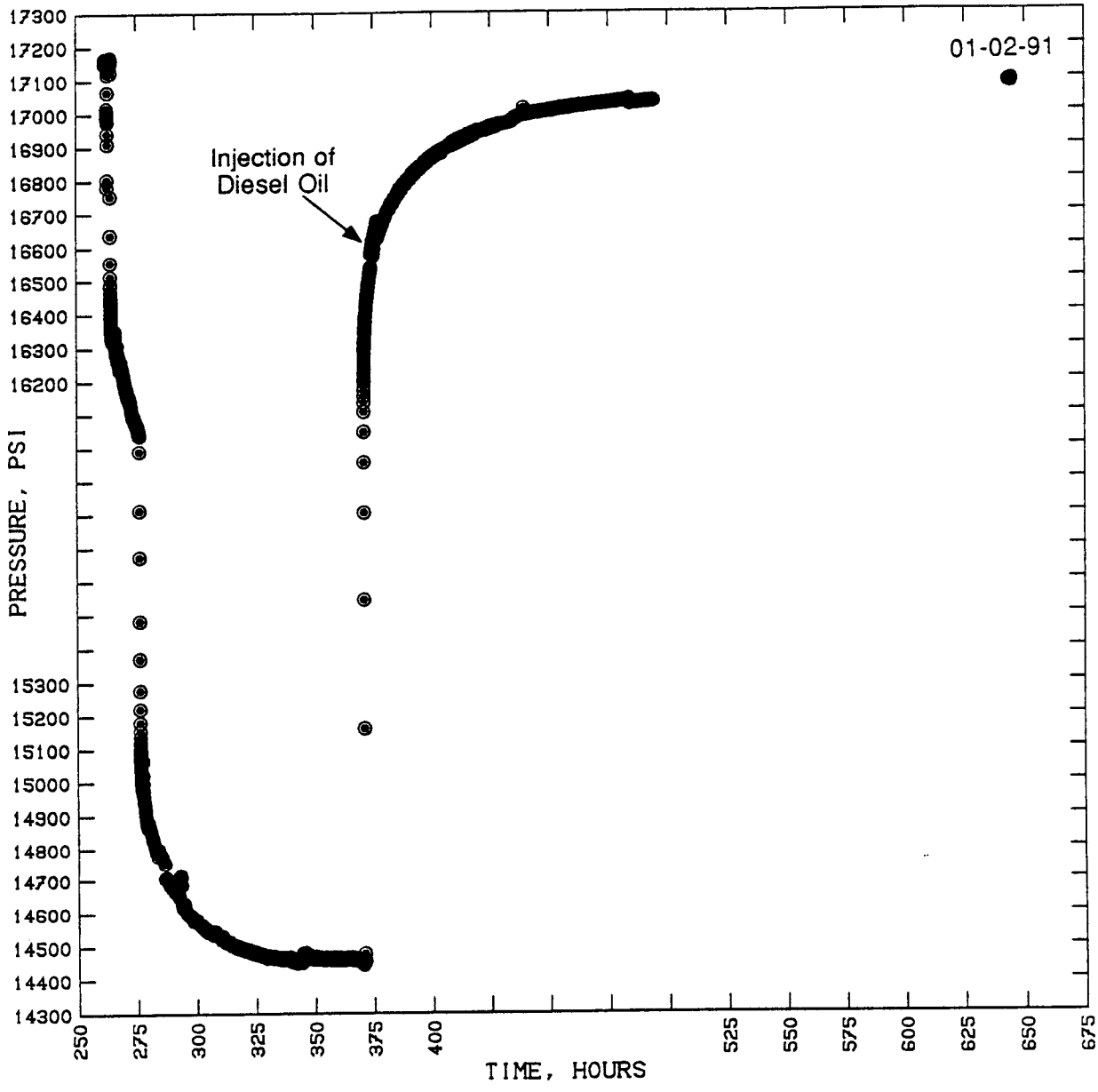

Figure 5. **Bottomhole pressure transient data from Flow Test No. 2; the data at ~ 644 hours were logged on January 02, 1990. Gauge at 20,525 feet depth.**

perforated and produced earlier. The occurence of internal crossflow between the two zones would complicate the interpretation of any new pressure transient data.

The test well was reopened on January 4, 1991 and flowed at rates varying from about 2,300 to 3,800 bbl/day, with a brief excursion to almost 5,000 bbl/dy before the well was shut on January 8. It was reopened on January 9 and flowed at an average rate of about 1,900 bbl/day, with a brief excursion to over 3,000 bbl/day, before finally being shutin on January 11, 1990. The production during Flow Test No. 3 is roughly approximated by the step flow rate history (January 4–11, 1990) listed in Table 2.

The measurements during January 4–8 by IGT appear to exhibit an increase in the gas/brine ratio as the flow rate is increased. When q was steady at ~ 3,200 bbl/day the value of GWR was ~ 31–32 SCF/STB. At ~ 5,000 bbl/day the GWR rose to ~ 35 SCF/STB. IGT concluded that the data were insufficient to determine to what extent the changes are due to hydrocarbon gases or carbon dioxide, and to what extent the variations reflect flow rate measurement errors (Randolph and Rogers, 1989–1990).

4. FLUID AND FORMATION PROPERTIES

The salinty of the produced fluid has been estimated to be approximately 180,000 to 198,000 mg/L and IGT concludes that the Hulin reservoir is fully saturated with natural gas. In contrast, both Gladys McCall and Pleasant Bayou fluids are unsaturated. The produced free gas is about fifteen percent carbon dioxide. To estimate fluid properties we have used an equation-of-state for brine/methane mixtures with the following mass fraction composition:

$$H_2O: 0.81640, \qquad CH_4: 0.00360, \qquad NaCl: 0.18000\ .$$

According to the equation-of-state (Pritchett, 1985a), this choice corresponds to a gas-to-water ratio (GWR) of 33.85 SCF/STB which falls within the range reported by IGT. For the initial reservoir conditions at 20,600 feet (17,308 psia, 342°F) the equation-of-state for the assumed composition yields estimates for the fluid viscosity (μ) and formation factor (B),

$$\mu = 0.294 \text{ cp}, \qquad B = 1.054 \text{ res bbl/stb bbl}\ .$$

The formation factor is required to convert stock tank barrels to reservoir barrels (at 20,600 feet datum).

In the absence of more definitive information for the Hulin formation, we will use the following values for the porosity (ϕ) and total formation compressibility (C_T):

$$\phi = 0.18 \qquad C_T = 4.83 \times 10^{-6}\ \text{psi}^{-1}.$$

The choice for ϕ lies near the center of the range (0.15 to 0.20) given by Dunlap (1989) based on logging operations at the Hulin well. The value for C_T is considered to be representative for geopressured sandstones.

5. PROXIMAL CONNECTED PORE VOLUME ESTIMATE

Table 4 summarizes static downhole pressure measurements corrected to a common datum level of 20,600 feet (35.625 psi is added to data recorded at 20,525 feet); the time the well had been shutin at the time of the measurement is also listed. Figure 6 is a plot of these pressure values against the total production at the time of measurement (including the November 20, 1989 cleanup flow of ~ 1,000 bbls). Only shutin times prior to the measurements on November 20, 1989, December 05, 1989 and January 02, 1990 are long enough for the data to approximate stable reservoir pressures; the latter two data points fix the lower line in Figure 6. The intercept of the line at $P_0 = 17{,}302$ psia is only 8 psi below the value recorded on November 20, 1989; this is well within measurement error. Its slope ($m^* \sim 7.45 \times 10^{-3}$ psi/bbl) represents the rate of decrease in the stable pressures in the deepest sand package (sand 1) when production is only from that sand. The shutin times for the other data in Table 4 are not long enough for sand 1 to attain stable pressures; these three data points fall below the solid line in Figure 6.

The correction is for a static column of water, but a gas pressure column. Is that correct?

Table 4. Bottomhole shutin pressures measured in Willis Hulin Well No. 1. (Datum level is 20,600 feet).

Date	Shutin Time (hours)	Q + 1,000 (barrels)	Pressure (psia)	Comment
11-20-89	~10^4	0.	17,308	stable
12-05	~340	1,000.	17,294	stable
12-10	50.6	4,658.	17,208	
12-17	83.7	7,680.	17,193	
12-27	123.0	23,537.	17,068	
01-02-90	380.0	23,537.	17,126	stable
01-03	[shallowest sand package perforated]			

The value of m^* can be used to estimate the proximal connected pore volume of sand 1:

$$V_1 = V\phi \sim \frac{1}{(m^* C_t)} = \frac{10^9}{(7.45)(4.83)} = 2.78 \times 10^7 \text{ bbls} \quad .$$

27,800,000

Under the working assumption that all six of the sand packages have the same porosity and areal extent, the estimate for the proximal connected pore volume of the total target sand sequence would be

stable :

unstable :

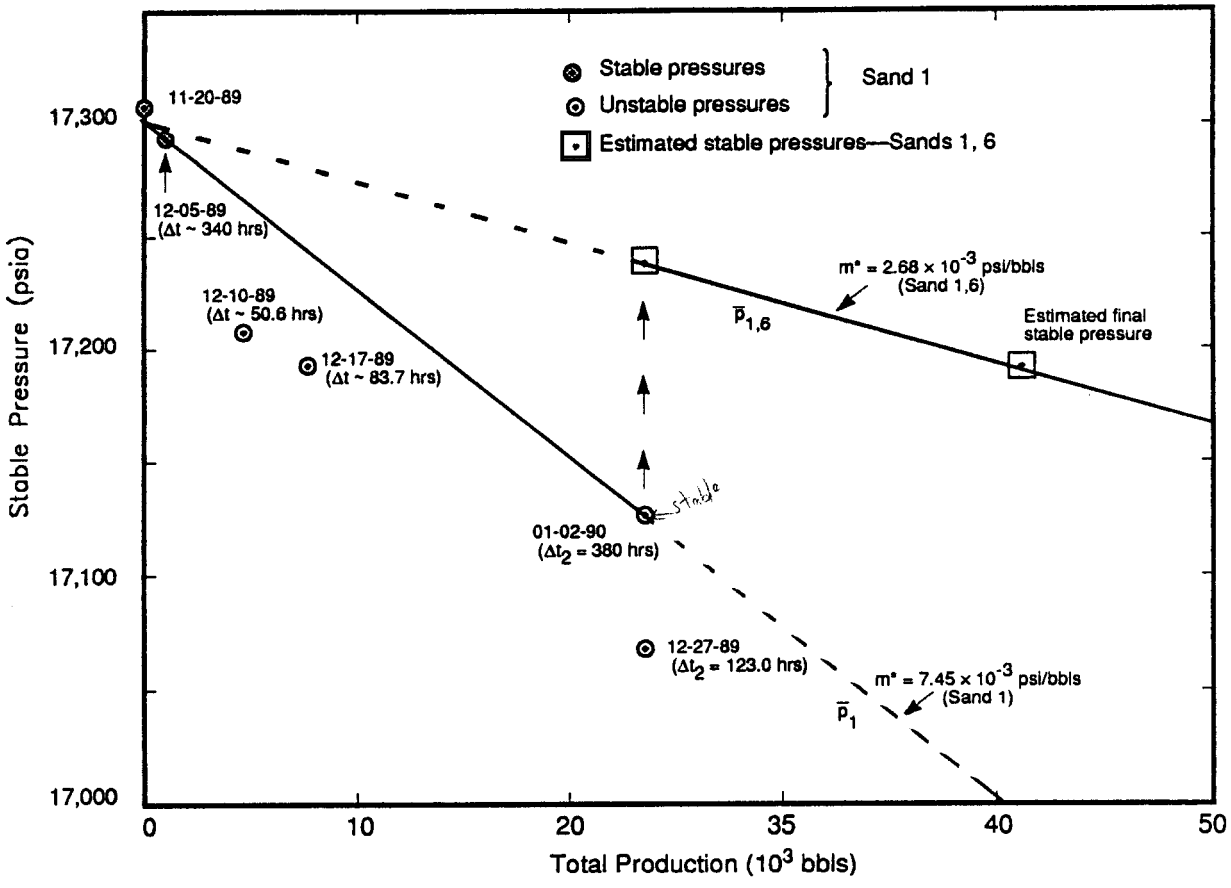

Figure 6. **Stable pressures at 20,600 feet depth versus total production from Willis Hulin Well No. 1. Transition from lower to upper line associated with perforation of sand 6.**

$$V_{total} = V\phi \sim \frac{470}{74} \times (2.78 \times 10^7) = 1.77 \times 10^8 \text{ bbls} \quad .$$

The corresponding estimate for the combined proximal connected pore volume of the shallowest and deepest sand packages (sands 1 and 6) would be

$$V_{16} = V\phi \sim \frac{206}{74} \times (2.78 \times 10^7) = 7.74 \times 10^7 \text{ bbls} \quad .$$

This volume implies that the stable pressure in the reservoir consisting of sands 1 and 6 would decrease from P_0 = 17,302 psia along a line of slope

$$m^* = \frac{74}{206} \times (7.45 \times 10^{-3}) = 2.68 \times 10^{-3} \text{ psi / bbl} \quad .$$

if both sands had been perforated from the outset of production. At the time that sand 6 was perforated on January 03, 1990 and wellbore communication established between the two sands, 23,537 bbls had been produced from sand 1. The higher hydrostatic head in the unproduced sand would induce flow from sand 6 through the wellbore into sand 1. The combined two-sand reservoir could be expected to attain a stable pressure at 23,537 bbls that falls near the upper line as depicted in Figure 6. The estimated final stable pressure for sands 1 and 6 at the conclusion of the preliminary testing of the Hulin well, i.e. Q + 1,000 = 41,163 bbls, is

$$\bar{p}_{16} = P_0 - \frac{Q + 1{,}000}{C_T \times V_{16}} = 17{,}302 - \frac{41{,}163}{(4.83)(7.74)10} = 17{,}192 \text{ psia} \quad .$$

An estimate of the increase in the stable pressure that would be expected to accompany the perforation of sand 6 can be estimated from the relation between the connected pore volumes in communication with the wellbore just prior to and immediately after the perforation,

$$\Delta\bar{p}_{16} = \Delta\bar{p}_1 \frac{V_1}{V_1 + V_6} = (17{,}302 - 17{,}126)\frac{74}{306} = 63 \text{ psi} \quad .$$

Therefore,

$$\bar{p}_{16} - \bar{p} = (17{,}302 - 63) - 17{,}126 = 113 \text{ psi} \quad .$$

It is of interest to note that this estimate is compatible with the jump in the wellhead pressure of ~ 7590 – 7482 = 108 psi observed in the Hulin well on January 03, 1990.

6. PRESSURE TRANSIENT DATA ANALYSIS

Erratic wellhead and bottomhole pressure values recorded during the first day of the FT1 drawdown (see Figure 4) were attributed by IGT to partial obstruction of the choke by old drilling mud from the continuing cleanup of the perforations. Injection of diesel oil (to prevent the formation of hydrates) between three and six hours after starting the drawdown portion of FT2 and the change in flow rate after about twelve hours render the data from the drawdown portions of this test useless for determining formation properties. The buildup parts of both tests, however, provide useful data.

Production rates were maintained nearly constant prior to shutin for both buildup tests. The data will first be analyzed using the Miller-Dyes-Hutchinson (MDH) method. Multi-rate analysis in which the detailed production history is considered using a Horner plot will then be presented. Both methods are discussed by Earlougher (1977).

6.1 MDH METHOD OF ANALYSIS

Consider a well with radius r_w flowing under semi-steady state conditions at rate q for an equivalent production period t_p. If there is a step rate change (Δq) at time t_p, the associated sandface pressure change at time $t_p + \Delta t$ ($\Delta p = [p_w]_{t_p+\Delta t} - [p_w]_{t_p}$) is approximated by (in oilfield units; see Earlougher, 1977)

$$\frac{\Delta p}{\Delta q} = m'\left(\log \Delta t + \log \frac{k}{\phi \mu C_T r_w^2} - 3.23 + 0.87\, s\right) ,$$

where $m' = 162.6\ \mu B/kh$. If we assume that the fluid viscosity (μ), formation porosity (ϕ) and total compressibility (C_T) are known, a semi-logarithmic plot of pressure transient data can be used to estimate the values of transmissivity (kh) and skin factor (s). The slope m' yields kh and the intercept at $\Delta t = 1$ hr yields s,

$$s = 1.151\left\{\frac{1}{m'}\left[\frac{\Delta p}{\Delta q}\right]_{1\ \mathrm{hr}} - \log \frac{k}{\phi \mu C_T r_w^2} + 3.23\right\} .$$

Figure 7 compares plots of $\Delta p/\Delta q$ vs log Δt for the buildup portions of Flow Test No. 1 (rate change from ~ 2,423 to 0 b/d on December 08, 1989) and Flow Test No. 2 (rate change

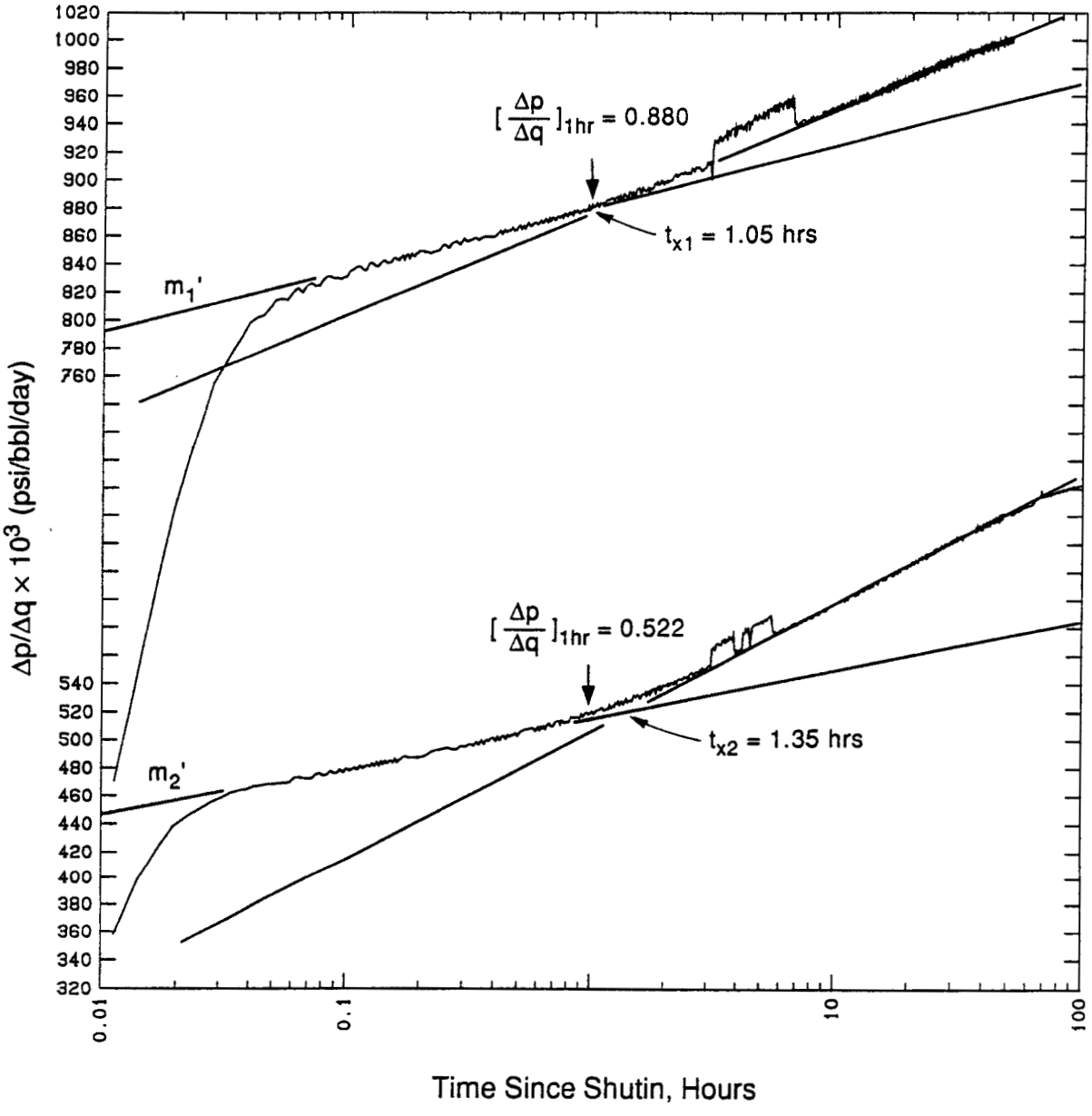

Figure 7. **Bottomhole pressure transient data from FT1 and FT2 buildup tests. Here the slopes are m1′ = 0.044 psi/cycle/bbl/day (FT1) and m2′ = 0.034 psi/cycle/bbl/day (FT2).**

from ~ 3,760 to 0 b/d on December 22, 1989). The early portions of the buildup curves are closely approximated by straight lines with slopes, respectively,

$$m1' = 0.044 \text{ psi/b/d} \quad m2' = 0.034 \text{ psi/b/d}.$$

The difference between these values are presumably due to errors in the flow rate data. The vertical displacement between the curves reflect changes in the skin factor between the times the tests were performed. The displacements in the two pressure buildup curves at $\Delta t = \sim 3$ to 7 hours in Figure 7 are caused by the injection of diesel oil into the test well.

We use the fluid/formation property values cited above ($\mu = 0.294$ cp, $B = 1.045$, $\phi = 0.18$ and $C_T = 4.83 \times 10^{-6}$ psi^{-1}) and $r_w = 0.252$ ft. Table 5 summarizes the calculations for the sand 1 tranmissivity and skin factor. The permeability values are based on the use of $h = 74$ feet, i.e., only the deepest sand package (20,616–20,690 feet) is assumed to be drained through the perforations in place at the time of these tests. The skin factor for FT2 ($s = 10.9$) is reduced from the value at FT1 ($s = 16.4$) by the additional perforations made on December 12–13, 1989. The skin factor remains large, however, since the 3.2-gram shaped charges that the small perforation gun carried could not penetrate far into the formation. The perforation intervals listed in Table 5 are nominal values; communication with the wellbore is probably less than indicated since some of the small charges may not have penetrated the wall of the 7-in casing.

Table 5 also lists the time (t_x) at which the slope of the straight line is approximately doubled during each buildup test (see Figure 7). This slope change is assumed to result from a hydrological barrier (e.g., a sealing fault) at a distance from the Hulin test well given by

$$L_x = 0.01217\sqrt{k\frac{t_x}{\phi\mu C_T}} \quad .$$

The estimates from FT1 and FT2 for the distance L_x (~ 97 to 125 feet) are listed in Table 5. It is apparent that the hydrological barrier is much closer to the well than the boundaries mapped as large growth faults in Figure 1. The mapped faults are over 3,000 feet away from the test well. Detailed study of any area often results in the identification of additional faults and other barriers to fluid flow.

6.2 MULTI-RATE TEST ANALYSIS

To account for the effects of flow rate variations prior to shutting a well for a buildup test, it is convenient to plot (see e.g. Earlougher, 1977) shutin pressure versus reduced time,

$$p_{ws} \text{ versus } \sum_{1}^{N}\frac{q_j}{q_N}\log\left\{\frac{t_N - t_{j-1} + \Delta t}{t_N - t_j + \Delta t}\right\} \quad .$$

Table 5. Summary of results of analysis of bottomhole pressure transient measurements during preliminary testing of Willis Hulin Well No. 1.

	Flow Test 1 Buildup	Flow Test 2 Buildup
Date of Measurement	Dec 08, 1989	Dec 22, 1989
Perforations, feet	20,670–20,690	20,602–20,690
Gauge Depth, feet	20,600	20,525
MDH Method of Analysis		
Δq, bbl/day	2,423	3,760
$[\Delta p/\Delta q]_{1\ hr}$, psi/bbl/day	0.880	0.522
m', psi/cycle/bbl/day	0.044	0.034
kh, md-ft	1,145	1,482
k, md	15.5	20.0
s	16.4	10.9
t_x, hours	1.05	1.35
L_x, feet	97	125
Multi-Rate Test Analysis		
m', psi/cycle	115	129
kh, md-ft	1,051	1,453
k, md	14.2	19.6
s	14.8	10.4
t_x, hours	2.0	1.0
L_x, feet (distance to barrier)	128	107

In an infinite acting reservoir, the plot should approximate a straight line with slope $m' = 162.6\ \mu B/kh$. The slope m' yields kh and the skin factor is calculated from the relation

$$s = 1.151\left\{\frac{p_{1\text{ hr}} - p_{wf}}{m'} - \log\frac{k}{\phi\mu C_T r_w^2} + 3.23\right\} \quad .$$

Figures 8 and 9 present such plots for Flow Test Nos. 1 and 2, respectively (at datum level 20,600 feet). The early portion of the plots are closely approximated by straight lines with slopes

$$m1' = 115 \text{ psi/cycle} \quad m2' = 129 \text{ psi/cycle.}$$

Using the relation $kh = 162.6\ \mu B/m'$, the corresponding estimates for the values of kh and k of sand 1 from Flow Test Nos. 1 and 2 (listed in Table 5) are essentially the same as estimated by the MDH method. Further, when the above relation for s is employed, the values calculated are very close to those computed by the MDH method.

To estimate the distance to the nearest hydrological barrier, straight lines with slopes double the infinite reservoir line slopes are shown in the figures. The lines intersect at buildup times (t_x) listed in Table 5. The corresponding estimates for the distance from the Hulin well to the nearest barrier are listed in the table for FT1 and FT2. The four estimates for the distance fall in a rather narrow range, $L_x \sim 97$ to 128 feet.

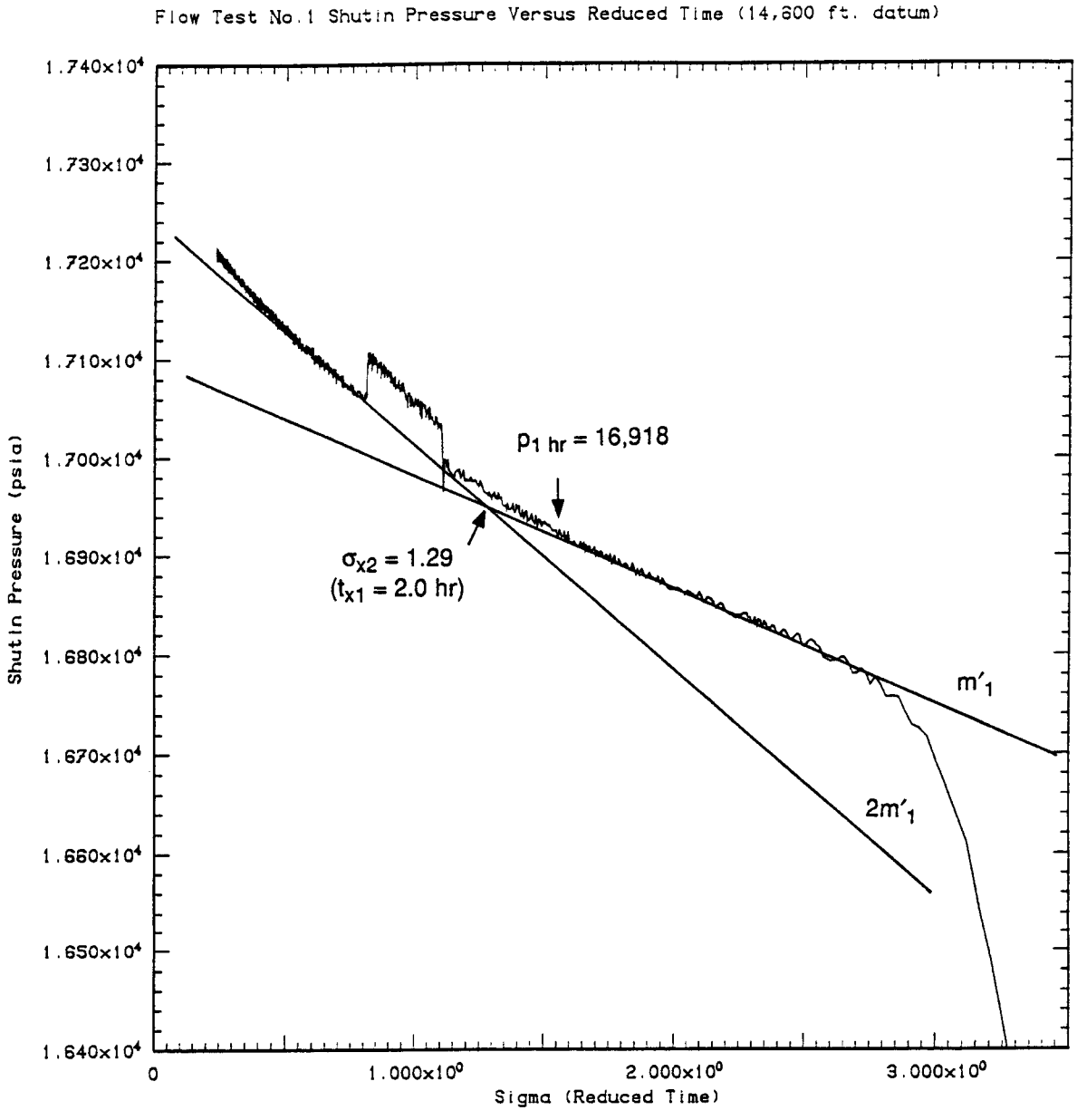

Figure 8. Bottomhole pressure transient data versus reduced time for FT1. Datum level is 20,600 feet.

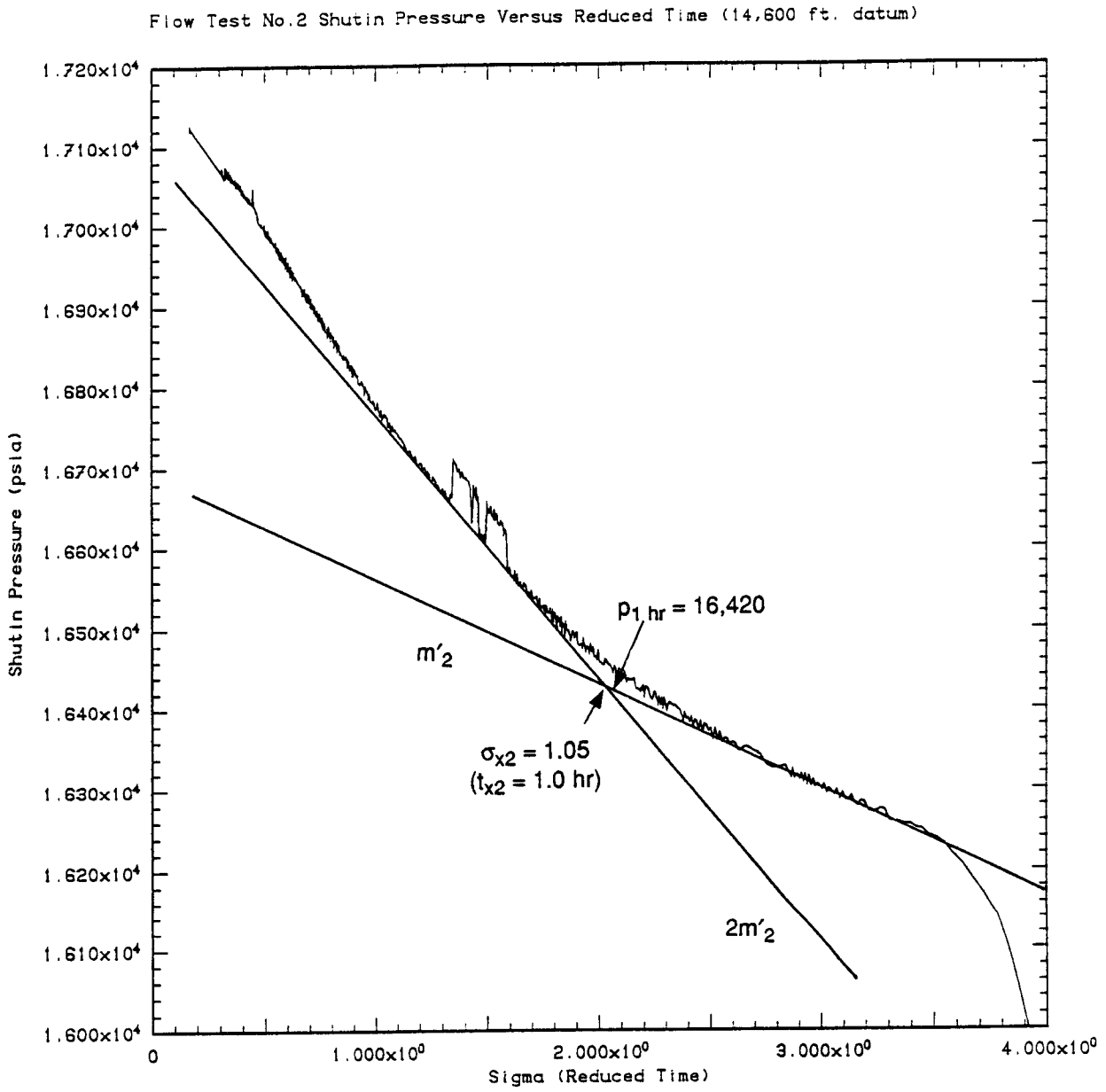

Figure 9. **Bottomhole pressure transient data versus reduced time for FT2. Datum level is 20,600 feet.**

7. WELLBORE CALCULATIONS

No bottomhole pressure measurements were made in the Hulin well subsequent to perforating the upper sand package (sand 6) on January 3, 1991. During the remainder of the flow testing (Flow Test No.3), commingled flow from sands 1 and 6 occurred with only wellhead data recorded. To attempt to evaluate the properties of sand 6 we will first need to estimate the pressure drop in the wellbore in order to estimate bottomhole pressures from wellhead values. A wellbore flow simulation model (Pritchett, 1985b) was used for this purpose.

Starting with specified bottomhole conditions, the program integrates up the well to predict the wellhead conditions. Frictional effects in the wellbore are treated using a correlation due to Duckler, *et al.* (1964); the effects of casing/tubing roughness are included through a relative roughness parameter (R) which is a model input parameter. Heat loss by combined conduction and convection from a porous water-saturated medium is treated by an effective formation conductivity (K). The wellbore model uses the equation-of-state for the Hulin brine, described above, to calculate the properties of the fluid as it rises in the casing/tubing completion configuration (Figure 2). The far-field temperature/depth profile was assumed to be the same as the stable profile measured during the pre-test logging of the Hulin well (Figure 3a).

The parameters R and K were varied in a series of iterative calculations with the wellbore model to determine those values which provide the best match to the recorded wellhead P/T data at times when stable P/T measurements were simultaneously being made downhole. The available calibration data consists of measurements made just prior to shutin during Flow Test Nos.1 and 2. The P/T data are best matched (for the assumed fluid composition and reservoir temperature, T_0 = 342°F) with the following values for the empirical parameters: K = 1.3 W/m^2 °C, R = 0.09 mm. These values provide good matches for the wellhead pressures; the calculated wellhead temperatures are somewhat higher than recorded since the drawdown tests were not long enough to attain temperature equilibrium.

Using these values of K and R, the calibrated wellbore model was then employed to estimate the pressure drop from the datum level (20,600 feet) to the wellhead as a function of flow rate (Figure 10). In particular, calculated drops (Δp) are listed in Table 6 for four times during Flow Test No.3 when relatively stable flow conditions were attained. The listed values for the flowing bottomhole pressures are obtained by adding the Δp values to the corresponding recorded wellhead pressure values.

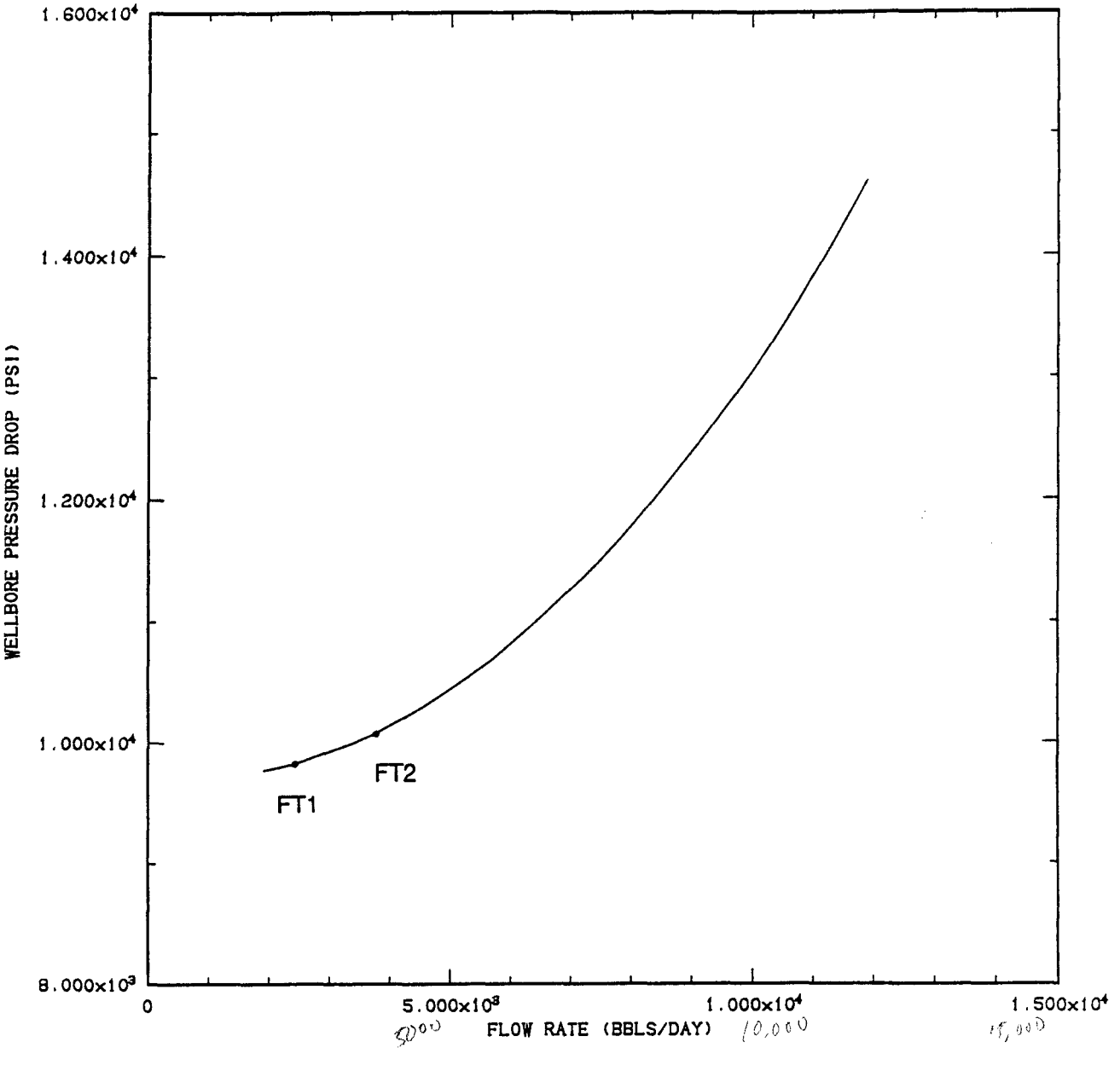

Figure 10. Pressure drop in Hulin wellbore from datum level (20,600 feet) to wellhead. Curve calculated with wellbore model calibrated using data from Flow Test Nos. 1 and 2.

Table 6. Estimated bottomhole pressures in Hulin well during Flow Test No. 3. (Datum level is 20,600 feet).

Test Day	Date	Time	Elapsed Time (hours	Q (bbls)	q (bbl/d)	WHP (psia)	Δp (psi)	BHP (psia)
32	1-06-90	15:00	742.1778	30,288	3,445	6,727	10,010	16,737
33	1-07	15:00	766.1778	32,879	2,440	7,000	9,832	16,832
34	1-08	15:00	790.1778	36,691	3,812	6,569	10,095	16,664
37	1-11	05:00	852.1778	40,163	1,910	7,250	9,775	17,025

8. RESERVOIR SIMULATION CALCULATIONS

8.1 MODEL LIMITATIONS

From the foregoing analysis of the pressure transient data, it appears that the distance from the Hulin well to the nearest hydraulic barrier is only about $L_x \sim 90$ to 130 feet, and that there is a second barrier (at distance L_y) which is much closer than the mapped major growth faults (Figure 1). The proximal connected pore volume estimate for sand 1 indicates that the area of the reservoir is approximated by

$$A = \frac{V_1}{h\phi} = \frac{(2.78 \times 10^7)(5.615)}{(74 \times 0.18)} = 1.17 \times 10^7 \text{ ft}^2 \quad .$$

For simplicity, the areal geometry is assumed to be rectangular; the aspect ratio of the rectangle and the location of the Hulin test well with respect to the boundaries will then be selected on the basis of a series of preliminary parametric reservoir simulations of the production history prior to the onset of commingled flow from sands 1 and 6 on January 3, 1990.

The choice of a rectangular configuration is only one of many alternatives and is not meant to imply that the configuration approximates the actual reservoir geology. It is only used as a vehicle to construct a reservoir model that behaves similarly to the behavior of the actual Hulin reservoir during the preliminary flow testing. The model is employed to estimate the near well permeability of sand 6 using commingled flow data (sands 1 and 6) during Flow Test No. 3. More extensive testing and more definitive knowledge of the geology and fluid composition for the reservoir will be needed to develop a realistic model.

8.2 PARAMETRIC CALCULATIONS (Sand 1)

The reservoir simulations all employed the values for the fluid properties ($\mu = 0.294$ cp and $B = 1.045$), well radius ($r_w = 0.252$), and formation properties ($\phi = 0.18$ and $C_T = 4.83 \times 10^{-6}$) used above. In the sand 1 simulations, the choices of $k_1 = 19$ md and $h_1 = 74$ feet correspond to $kh = 1{,}406$ md-ft which is compatible with the analysis of the downhole pressure buildup data. The simulations used the production history approximation presented in Table 2.

Figure 11 illustrates the effects on the simulated Flow Test 2 pressure buildup history for six choices of the well/reservoir dimensional parameters. All six cases assume $A = X \times Y =$

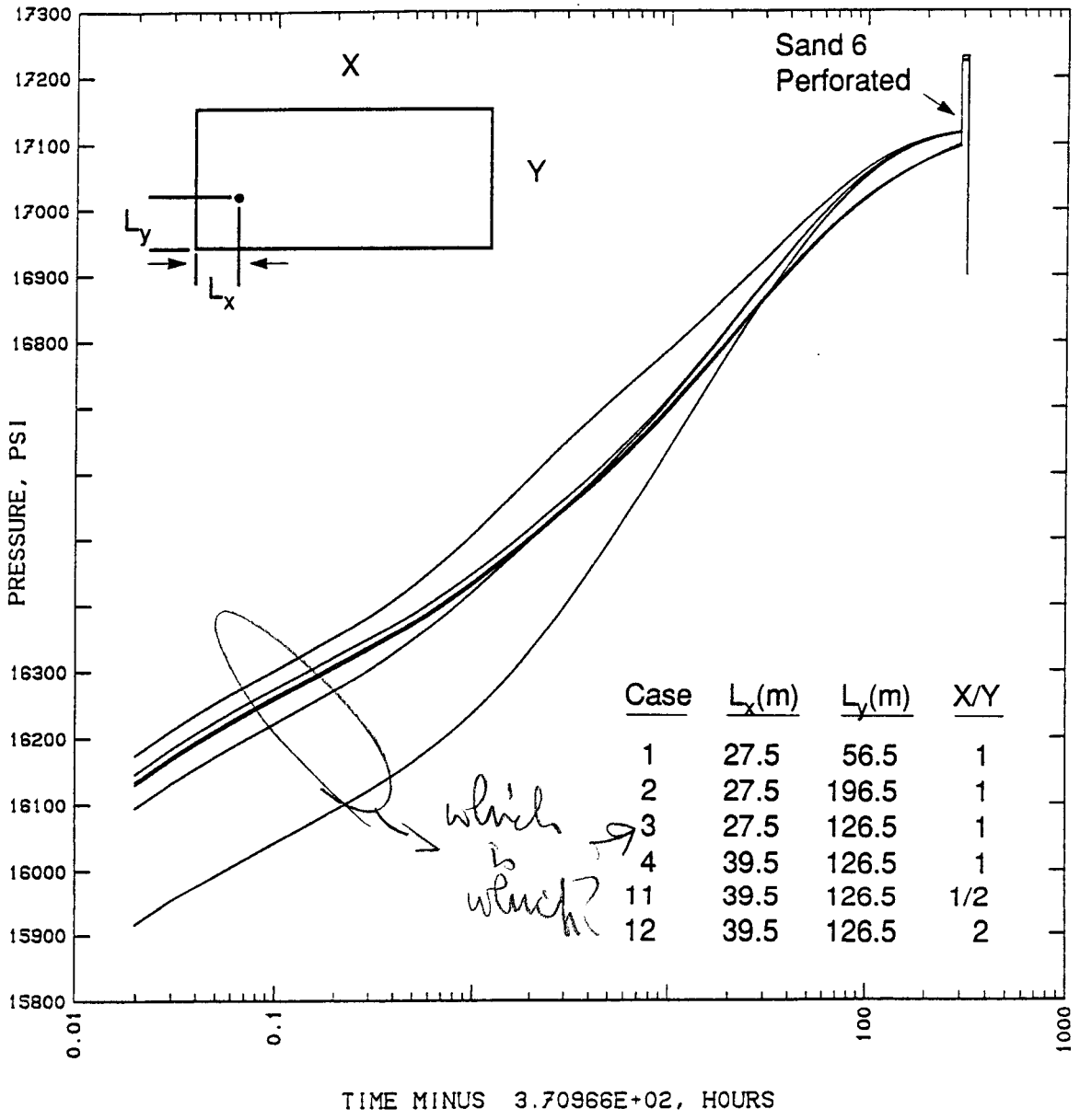

Figure 11. Effect of reservoir/well dimensional parameters on the calculated FT2 pressure buildup response for sand 1. Datum level is 20,600 feet.

1.20×10^7 ft^2, corresponding to the value estimated earlier for the proximal connected pore volume of sand 1. The first four cases assume the area is a square ($X = Y = 3{,}460$ feet) and vary L_x and L_y within the estimated range of values. The choice (case 4) which provides the best history match to the pressure buildup data ($L_x = 130$ feet; $L_y = 415$ feet) was then used in the last two simulations to evaluate the effect of the aspect ratio of the rectangular reservoir geometry. It is apparent from Figure 11 that the distances to the two more remote reservoir boundaries have very little effect on the simulated pressure history. Since the square geometry provides just as good agreement with the available data, it is selected for simplicity.

8.3 HISTORY MATCHING SIMULATIONS (Sands 1 and 6)

Using the well/reservoir geometry that provided a good match to the sand 1 test history (case 4 in Figure 11), a series of simulations were then performed for the full production history of the Hulin well as approximated in Table 2. To model the commingled flow subsequent to perforating sand 6 on January 3, 1990, it is required to specify values for the sand 6 formation parameters and to make assumptions regarding connectivity beween the sand packages. We have simply assumed that during the short-term testing the shale layers prevent any crossflow between the sands; commingled flow from the two perforated sands is presumed to occur only within the wellbore. The values of ϕ, C_T and proximal areal extent for sand 6 are assumed the same as for sand 1. The thickness of sand 6 is based on its its value at the wellbore ($h_6 = 132$ feet), and its permeability (k_6) was varied in series of parametric calculations.

Trial permeability values assigned included $k_6 = 19$, 25, 30, and 35 md. The four calculations are identical prior to the perforation of sand 6 since they employ the same parameters for sand 1. Figure 12 compares the calculations (from a time just prior to starting the commingled flow) with the estimated bottomhole pressures (listed in Table 6). In these four calculations, the effective skin factor (in both sands) during the commingled flow period was set at $s_{16} = 0$ for convenience. The calculation using $k_6 = 19$ md (same as k1) gives a good match to the first three points in Table 6 but not the fourth (estimated bottomhole pressure at $q = 1{,}910$ b/d on January 11, 1990). This value is incompatible with the other three points; it is about 125 psi too high. We assume that the value of Δp added to the recorded wellhead pressure is too large which would result from use of a value of q in the wellbore calculations that is too large. The IGT data report (Randolph and Rogers, 1989–1990) alludes to flow rate measurement problems after January 9, 1990 that resulted in the brine turbines reading high and the gas meter reading low.

Only the first three data points in Table 6 will therefore be considered. The choice of $k_6 = 19$ md is rejected since this match (Figure 12) corresponds to $s_{16} = 0$ (sand 1 exhibited a skin factor of $s_1 = 9$ during FT 2 and s_6 is unlikely to be negative since perforations of sand 6 were also done using small charges). The best match to the three credible estimates for the bottomhole pressure values in Table 6 is provided by the choices

$$k_6 = 25 \text{ md and } s_{16} = +3.0.$$

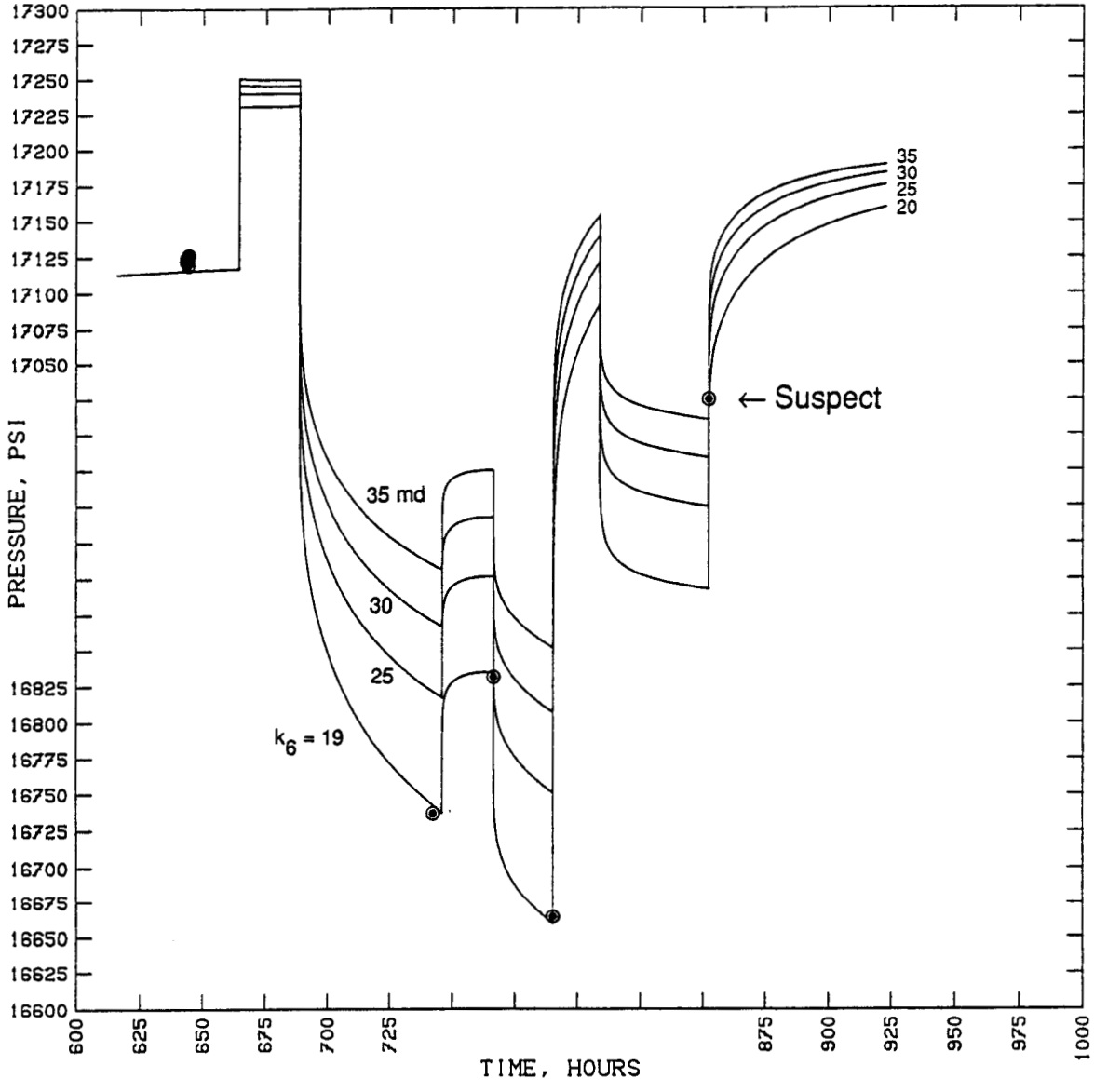

Figure 12. Effect of trial sand 6 permeability values on the calculated response during FT3 of the two-sand reservoir (sand 1 and sand 6).

With these choices and the proximal reservoir configuration/properties used in case 4, a satisfactory match to the complete test history is obtained. The simulated test history is compared with the total bottomhole data available in Figure 13. Detailed comparisons with the FT1 and FT2 bottomhole buildup data are also given (Figures 14 and 15).

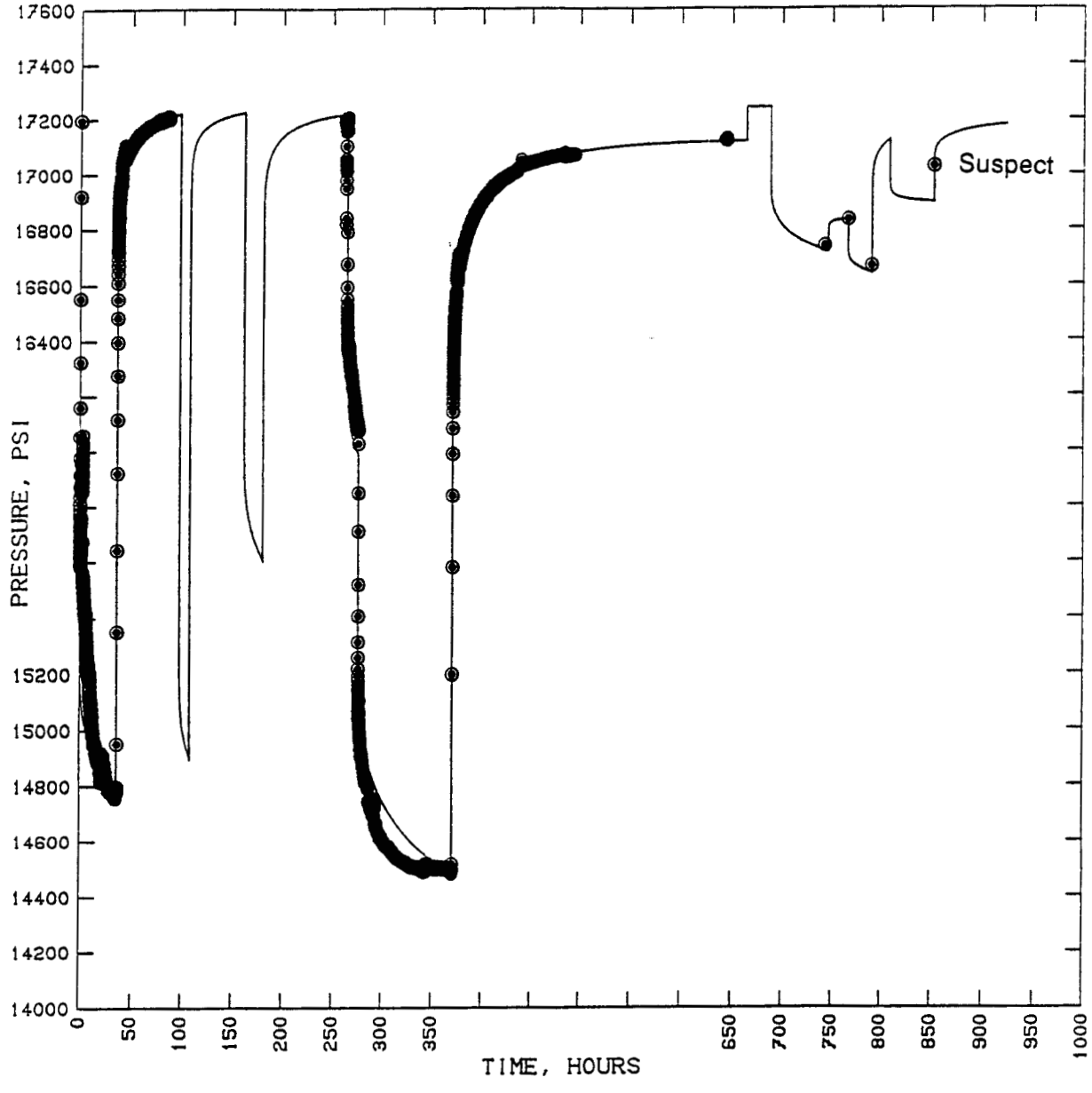

Figure 13. Comparison of simulated test history (curve, case 4) with composite bottomhole pressure data (points) from preliminary testing of Willis Hulin Well No. 1. Datum level is 20,600 feet.

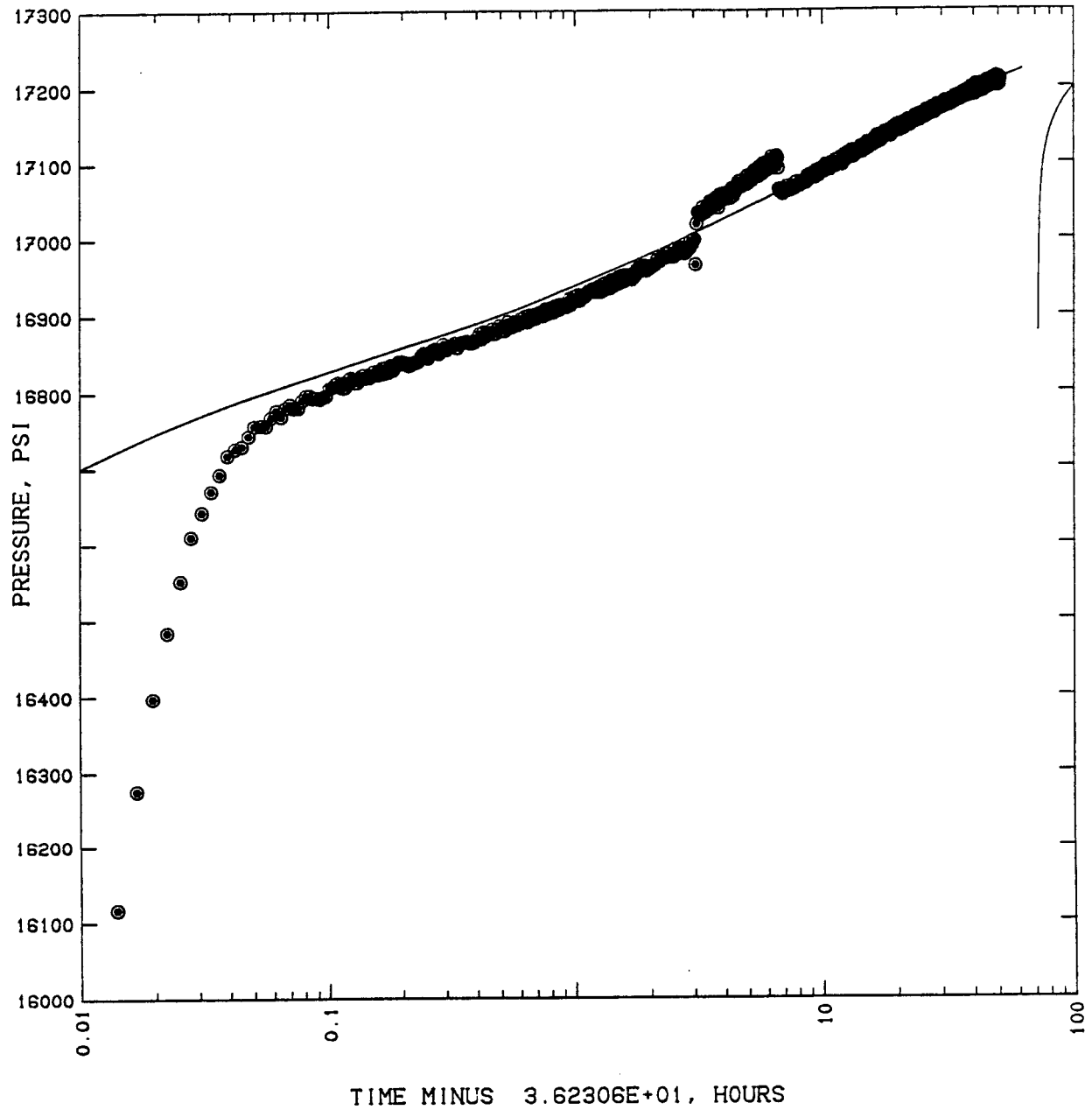

Figure 14. Detailed comparison of simulated FT1 pressure buildup history (curve, case 4) with bottomhole pressure buildup data (points) for Willis Hulin Well No. 1. Datum level is 20,600 feet.

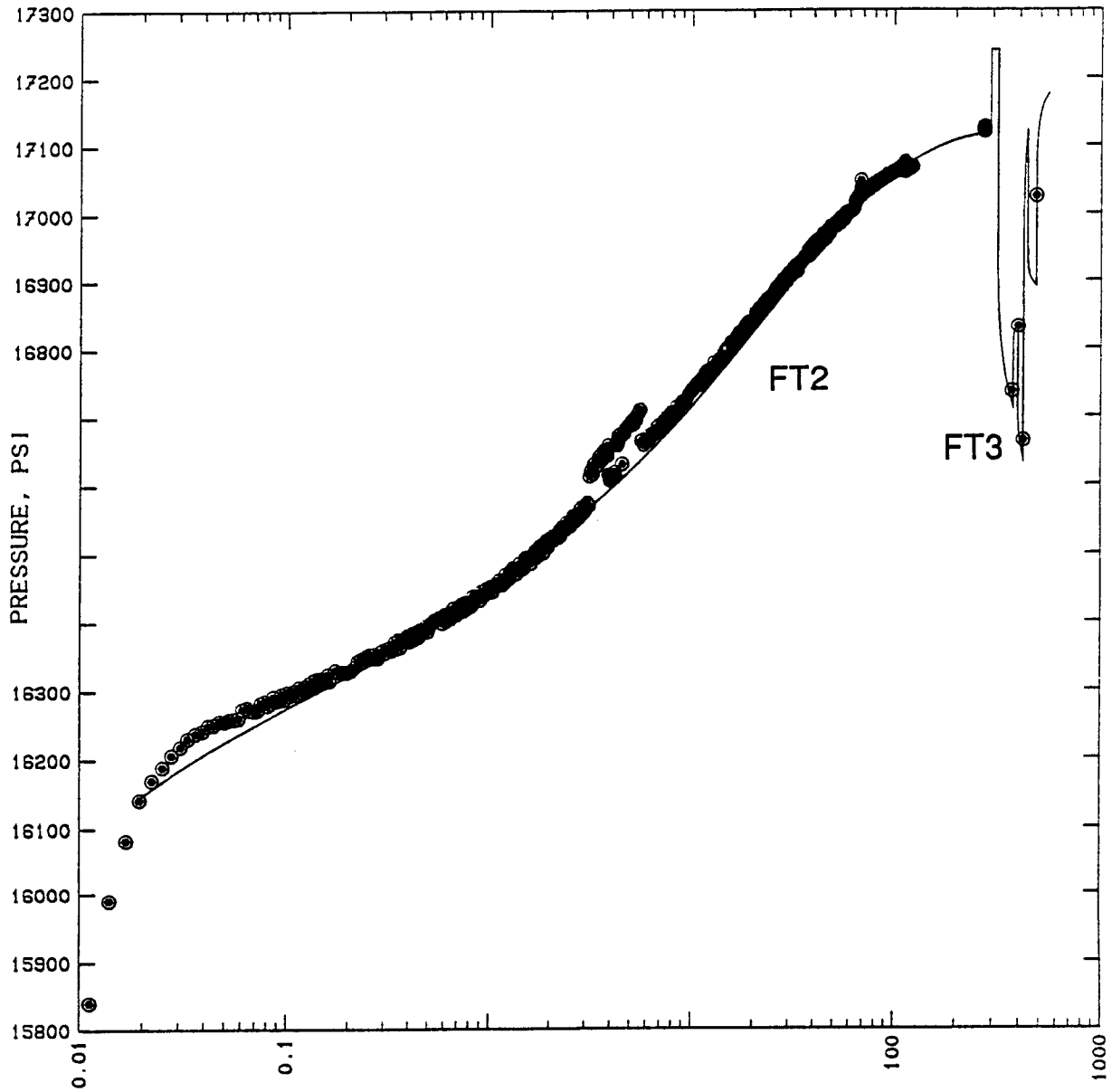

Figure 15. Detailed comparison of simulated FT2 pressure buildup history (curve, case 4) with bottomhole pressure buildup data (points) for Willis Hulin Well No. 1. Comparison with calculated FT3 downhole pressures are also shown. Datum level is 20,600 feet.

9. FUTURE TESTING OF HULIN WELL

9.1 MAJOR UNCERTAINTIES

Because of the very limited data base, conclusions from analysis of the preliminary flow testing are necessarily tenuous. It appears, however, that the formation permeability is about 15 to 25 md and that the proximal pore volume for the full target reservoir sand-shale sequence (20,220–20,690) is only about 180 million barrels. From analyses of long-term test data for the Gladys McCall (Riney, 1990) and Pleasant Bayou (Riney, 1991) geopressured reservoirs, however, we suspect there might be remote (poorly connected) reservoir volume that will provide long-term pressure maintenance at Hulin. The seismic map prepared by LSU (Figure 1) suggests a reservoir volume of at least one billion barrels. Nevertheless, it would seem prudent to flow the well for several months, even though constrained to low flow rates by existing plumbing, to better determine reservoir volume before committing to recompletion of the Hulin well. A six-months production test is suggested.

If information from the drilling and testing of the British Gas Exploration well becomes available it is likely to profoundly affect planning for long-term testing of the Hulin well. Inter-well interference data from wells completed in the same sand-shale sequence have not been available from any geopressured reservoirs previously tested by DOE. Lack of such data severely limits locating internal flow boundaries which might dominate reservoir response.

Another uncertainity is the presence or absence of a free gas reservoir in communication with the Hulin well. The produced fluid appears to be saturated at reservoir conditions but the gas content of *in situ* fluid is only approximately known. The response of the Hulin reservoir during the proposed six-months production test will depend strongly on the gas content, provided there is substantial free gas present.

9.2 PARAMETRIC CALCULATIONS (Sands 1 through 6)

To examine the sensitivity of the produced GWR to the reservoir gas content, a series of one-dimensional cylindrical calculations were made in which the mass fraction composition assumed at the original reservoir conditions (17,294 psia, 342°F) was varied from case to case. These parametric simulations employed the equation-of-state for brine/methane mixtures; the cases considered all assumed a NaCl mass fraction of 0.1800 but the CH_4 mass fraction was varied as listed in Table 7. The values of the corresponding calculated initial free gas saturations in the reservoir ($S_{g,o}$) are also listed.

Table 7. Methane content and relative permeability functions assumed in series of parametric calculations (brine NaCl mass fraction = 0.1800) and summary of case-by-case results.

Case No.	Frac. CH_4	Gas Sat. $S_{g,o}$	Pressure Drop (psi) Open (6 mo)	Pressure Drop (psi) Shut (12 mo)	m psi/~	k md	GWR (scf/bbl) resvr.	GWR (scf/bbl) $t = 0$	GWR (scf/bbl) $t = 6$ mo.
Martin's R_w and R_g curves: $S_{wr} = 0.35$, $S_{gr} = 0.05$									
a	0.0036	0.0002	1242	1046	28.1	18.9	33.85	33.20	32.14
b	0.0000	0.0000	1301	1108	27.9	19.1	0.00	0.00	0.00
c	0.0050	0.0054	1219	1020	28.9	18.4	47.12	33.14	32.10
d	0.0075	0.0146	1183	1030	30.2	17.6	70.92	33.22	32.04
e	0.0100	0.0236	1151	937	30.9	17.2	94.85	32.93	31.97
f	0.0150	0.0413	1098	869	33.5	15.9	143.14	32.72	31.85
g	0.0200	0.0586	1064	822	36.0	14.8	191.97	68.76	75.62
h	0.0250	0.0755	1048	789	37.6	14.1	241.38	146.02	155.31
i	0.0300	0.0920	1041	764	40.6	13.1	291.36	232.09	244.28
Martin's R_w and linear R_g curves: $S_{wr} = 0.35$, $S_{gr} = 0.30$									
a1	0.0036	0.0002	1242	1046	28.3	18.8	33.85	33.20	32.14
f1	0.0150	0.0413	1099	866	133.5	13.4	143.14	32.71	31.80
i1	0.0300	0.0920	1010	721	41.8	6.8	291.36	32.06	31.22
Martin's R_w and linear R_g curves: $S_{wr} = 0.35$, $S_{gr} = 0.10$									
a2	0.0036	0.0002	1244	1046	28.3	18.8	33.85	33.20	32.14
f2	0.0150	0.0413	1152	866	39.6	13.4	143.14	32.71	31.80
i2	0.0300	0.0920	1269	721	77.7	6.8	291.36	32.06	31.22

S_{wr} defn?

S_{gr} ~ trapped gas saturation

The reservoir formation properties were the same as used for Hulin sand 1 history matching simulations ($\phi = 0.18$, $C_T = 4.83 \times 10^{-6}$ psi^{-1}, $k = 19$ md). The calculations assume that the full thickness of the Hulin target sand/shale sequence will be perforated prior to long-term testing, $H = 470$ feet; the outer boundary of the reservoir was set at a radius of $R = 1955$ feet to approximate the total reservoir pore volume estimated from the flow test data,

$$H\phi(\pi R^2) = 470(0.18)\pi(1955)^2[0.178 \text{ bbl} / \text{ft}^3] = 1.8 \times 10^8 \text{ bbls} \quad .$$

In all cases the well ($r_w = 0.252$ ft) was produced from the fully penetrated reservoir thickness of 470 feet at a constant rate of 5,000 stb/d for six months; the well was then closed and the pressure buildup computed for six months. A flow rate of 5,000 stb/d should be possible with the present completion (3.5-inch tubing). The skin was set to zero ($s = 0$) for simplicity in these simulations for evaluating the effects of gas content. Reservoir response and GWR of the fluid produced from the Hulin well will be influenced by the gas content (CH_4 mass fraction) and relative permeabilities of the gas (R_g) and liquid (R_w) phases in the formation. Sparse laboratory data (Roberts, 1980) of relative permeabilities on several cores obtained from the Pleasant Bayou wells indicate that R_w declines with small amounts of free gas in the pores and $R_g < 0.0005$ for $S_g < 0.235$ (Figure 16). Sufficient data are, however, not available to firmly establish relative permeabilities. From experience in gas and oil reservoirs, Martin (1979) concludes that S_{gr} is at least 2 to 5 percent and suggests the relative permeability curves shown in Figure 16 for calculating produced GWR values. Garg, *et al.* (1986) used Martin's curves with $S_{wr} = 0.35$ and $S_{gr} = 0.050$ in parametric calculations for brine and gas recovery from geopressured reservoirs. Here we first use Martin's original curves for illustrating the effects of CH_4 mass fraction on produced GWR (cases a through i in Table 7). Because of the larger effects implied by Roberts data, however, we have also used a revised version of Martin's Rw curve and examined the effects of much larger values of S_{gr} using a linear function for R_g (Figure 17).

Table 7 summarizes the results of the series of parametric calculations. (More descriptions of the parametric calculations are given in the Appendix.) In all cases treated, the produced GWR (from $t = 0$ to 6 mo.) is less than the reservoir GWR. When there is an immobile free gas phase ($S_g < S_{gr}$) at the sandface, the produced GWR slowly declines with reduction in the sandface pressure since the solubility of CH_4 decreases with pressure. The slow decline in produced GWR in these cases (a,c,d,e,a1,f1,i1,a2,f2), and cases (f,i2) where only a small amount of free gas is produced, might not be discernable in practice since flow rates can not be kept constant for extended periods. If there is a mobile free gas phase from the outset (cases g,h,i), however, it would be apparent from the much larger produced GWR.

For higher free gas saturation in the reservoir,the fluid (and total formation) compressibility is higher. Consequently, the pressure near the sandface during production ($t < 6$ mo) and the final pressure after six months of shutin ($t = 12$ mo) are larger. Table 7 lists the pressure drop from the original reservoir value (17,294 psia) at these points in time for each of the cases considered.

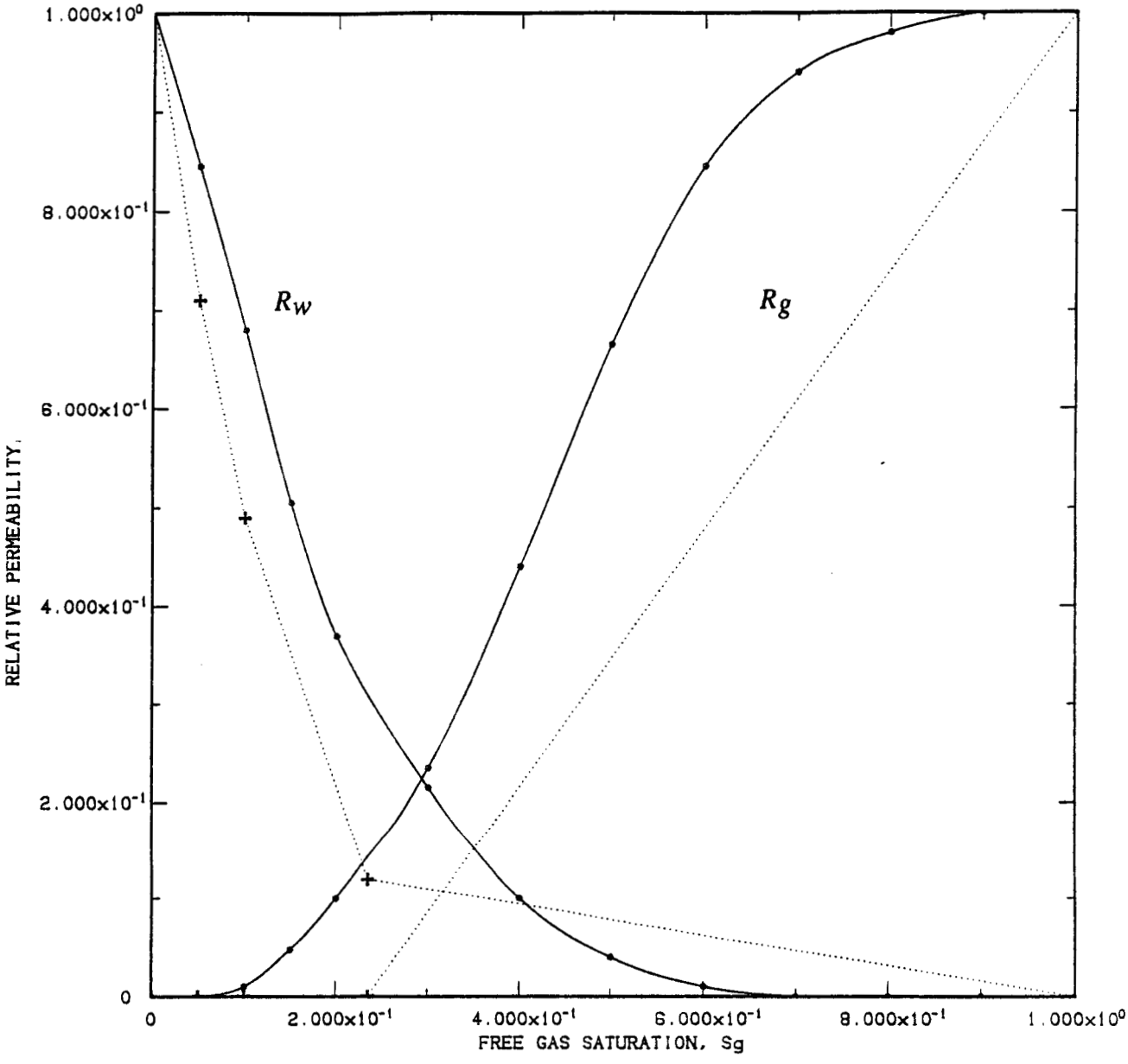

Figure 16. Comparison of original Martin relative permeability functions (solid line curves) with measurements by Roberts (+).

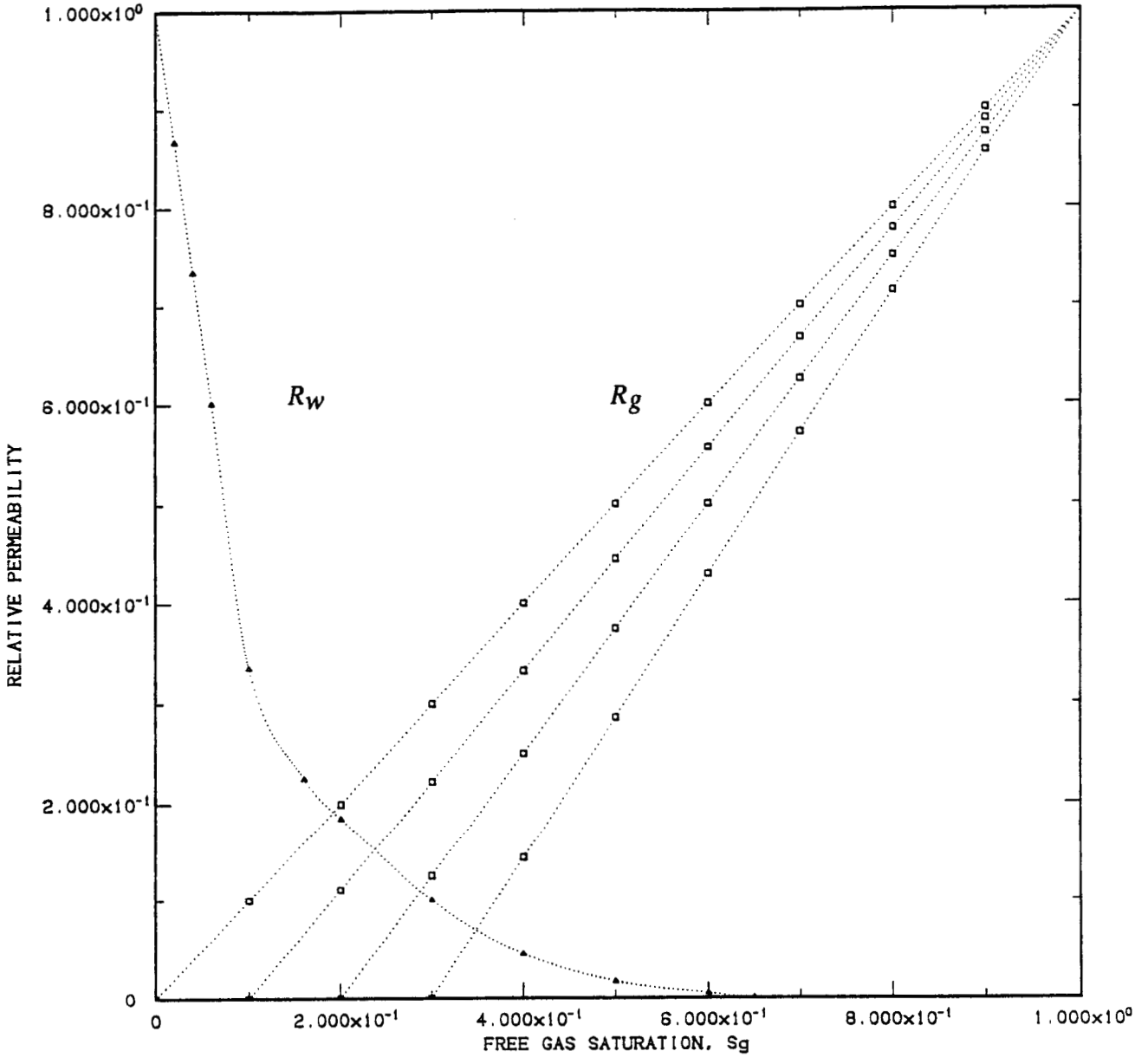

Figure 17. Revised Martin R_w curve and various linear R_g functions (for S_{gr} = 0.0, 0.1, 0.2 and 0.3).

Table 7 also lists the values of the slopes of the pressure buildup curves and the corresponding values of formation permeability that would be inferred from conventional analysis. It is of interest to note that large reductions in inferred k values (e.g. cases f2 and i2) can occur at produced GWR values that are non-distinguishable from those calculated for much lower CH_4 mass fraction (case a). The implied skin factors ($|s| < 2$, not listed in Table 7) are small.

10. REFERENCES

Bebout, D. G., Z. Bassiouni, D. R. Carver, C. G. Groat, A. E. Johnson, Jr. and F. M. Wrighton (1982), "Technical Support for Geopressured-Geothermal Well Activities in Louisiana," Annual Report under U.S. Department of Energy Contract No. DE-AC08-81NV10174, October.

Dukler, A. E., M. Wicks III and R. G. Cleveland (1964), "Frictional Pressure Drop in Two-Phase Flow-B: An Approach Through Similarity Analysis," *A.I. Ch. E. J., Vol. 10*, pp. 44.

Dunlap, H. F. (1989), "Logging Operations at Hulin Well and Preliminary Interpretation of Results", Trip Report, University of Texas at Austin, Petroleum Engineering Department, January 18.

Earlougher, R. C., Jr. (1977), "Advances in Well Test Analysis", Monograph No. 5, Society of Petroleum Engineering of AIME, Dallas, Texas.

Eaton, B. A., T. E. Meahl and C. R. Featherstone (1990), "Department of Energy (DOE) Geopressured-Geothermal Program Workover and Recompletion Operations: Willis Hulin Well No. 1, Vermilion Parish, Louisiana", Manuscript prepared for publication.

Garg, S. K., T. D. Riney and R. H. Wallace (1986), "Brine and Gas Recovery from Geopressured Systems", Geothermics, Vol. 15, pp. 23–48.

Hamlin, H. S. and N. Tyler (1988), "Consolidation of Geologic Studies of Geopressured-Geothermal Resources in Texas," Annual Report under U.S. Department of Energy and The University of Texas at Austin Cooperative Agreement No. DE-FC07-85-NV1041, December.

John, C. J. (1991), "Hulin Prospect Geology," Section in Louisiana State University Report for the period 1 December 1988–31 Decembr 1990, U. S. Department of Energy Contract DE-FC07-85NV10425, pp. 97–115, July.

Martin, J. C. (1979), "A Study of Simultaneous Production of Water and Gas from Aquifers Containing Initial Immobile Free Gas", Society of Petroleum Engineering Paper No. 8356.

Pritchett, J. W. (1985a), " 'CH4BRN': A New Geopressure Equation-of-State for the 'THOR' Reservoir Simulator", S-Cubed Report SSS-IR-86-7589 (October).

Pritchett, J. W. (1985b), "WELBOR: A Computer Program for Calculating Flow in a Producing Geothermal Well", S-Cubed Report SSS-R-85-7283 (Revised July 1986).

Randolph, P. L. and L. A. Rogers (1989), "Hulin Wireline Logging and Hydrates", IGT Memorandum to File, November 30.

Randolph, P. L. and L. A. Rogers (1989–1990), "Willis Hulin Production Data Reports", August 1989, November 1989 and weekly from December 2, 1989 through January 12, 1990.

Riney, T. D. (1990), "Depletion and Recovery Behavior of the Gladys McCall Geopressured-Geothermal Reservoir", S-Cubed Report SSS-TR-90-11474.

Riney, T. D. (1991), "Pleasant Bayou Geopressured-Geothermal Reservoir Analysis—January 1991", S-Cubed Report SSS-TR-91-12162.

Roberts, B. W. (1980), "Relative Permeability Measurements of Texas Gulf Coast Sandstones at Low Free Gas Saturations", Center for Earth Sciences and Engineering—Division for Rock Mechanics, The University of Texas at Austin, Austin, Texas, Report No. UT 80-2.

APPENDIX

The reservoir fluid in case b (see Table 7) has no methane content. For cases a, c, d, e, the free gas saturation remains less than $S_{gr} = 0.050$ for the full 6 months of production at 5000 stb/d. Free gas accumulates in the neighborhood of the wellbore over the 6 month drawdown period (Figure A.1); there is no movement of the free gas phase. The increase in S_g (greatest for case e) increases the fluid (and total formation) compressibility. Consequently, the rate of pressure decline decreases (Figure A.2). The produced CH_4 (and GWR) corresponds to the saturation value at the sandface pressure at that point in time. Since the solubility of CH_4 declines slowly with pressure, the produced GWR declines slowly with time of production (Figure A.3). The increase in S_g near the well reduces the liquid phase relative permeability (R_w) somewhat as reflected by the small increase in the slope of the pressure buildup curves (Figure A.4). The slope for case e is about 11 percent greater than for case b; the implied value of the permeability (k) for case e is correspondingly 11 percent lower (see Table 7).

In cases g, h, i free gas saturation is greater than $S_{gr} = 0.050$ initially and free gas flows into the wellbore from the outset of production. Since the mobility of the gas phase is less than that of the liquid phase in the applicable range of S_g, the produced GWR is less than the GWR of the reservoir fluid; consequently, S_g in the vicinity of the well increases with increasing drawdown time (Figure A.5). The increase in S_g (greatest for case i) increases the total reservoir compressibility and the pressure decline rate is therefore decreased (Figure A.6). As the value of S_g increases, the ratio of gas mobility to water mobility also increases (Figure 16) and the GWR of the produced fluid increases with time (Figure A.7). The increase in S_g near the wellbore reduces the liquid phase mobility which is reflected by the increase in slope of the pressure buildup curves (Figure A.8). The implied k value for case i is about 31 percent less than for case b.

For case f the near-sandface value of S_g increases from $S_{g,o} = 0.0413$ to $S_{gr} = 0.050$ at about 120 days of production (Figure A.1). There is a very small amount of free gas produced thereafter. Results for cases f, f1, f2, are shown together to illustrate the effects of changes in the relative permeability functions. No free gas flows in cases f1 and f2 since the assumed values of S_{gr} are not attained. The pressure responses for cases f and f1 are essentially identical since R_w is unchanged and R_g is very small; the revised Martin R_w curve employed in case f2, however, significantly reduces the liquid phase permeability in case f2 (Figures A.6 and A.8). The produced GWR for the three cases would be indistinguishable (Figure A.3).

Cases i, i1, i2 illustrate the effects of changes in the relative permeability functions for a much higher CH_4 mass fraction; the initial free gas saturation is $S_{g,o} = 0.0920$. For the original Martin R_w and R_g functions free gas is produced from the outset of drawdown (case i, Figure A.7); the near well free gas saturation increases slowly with production time as shown

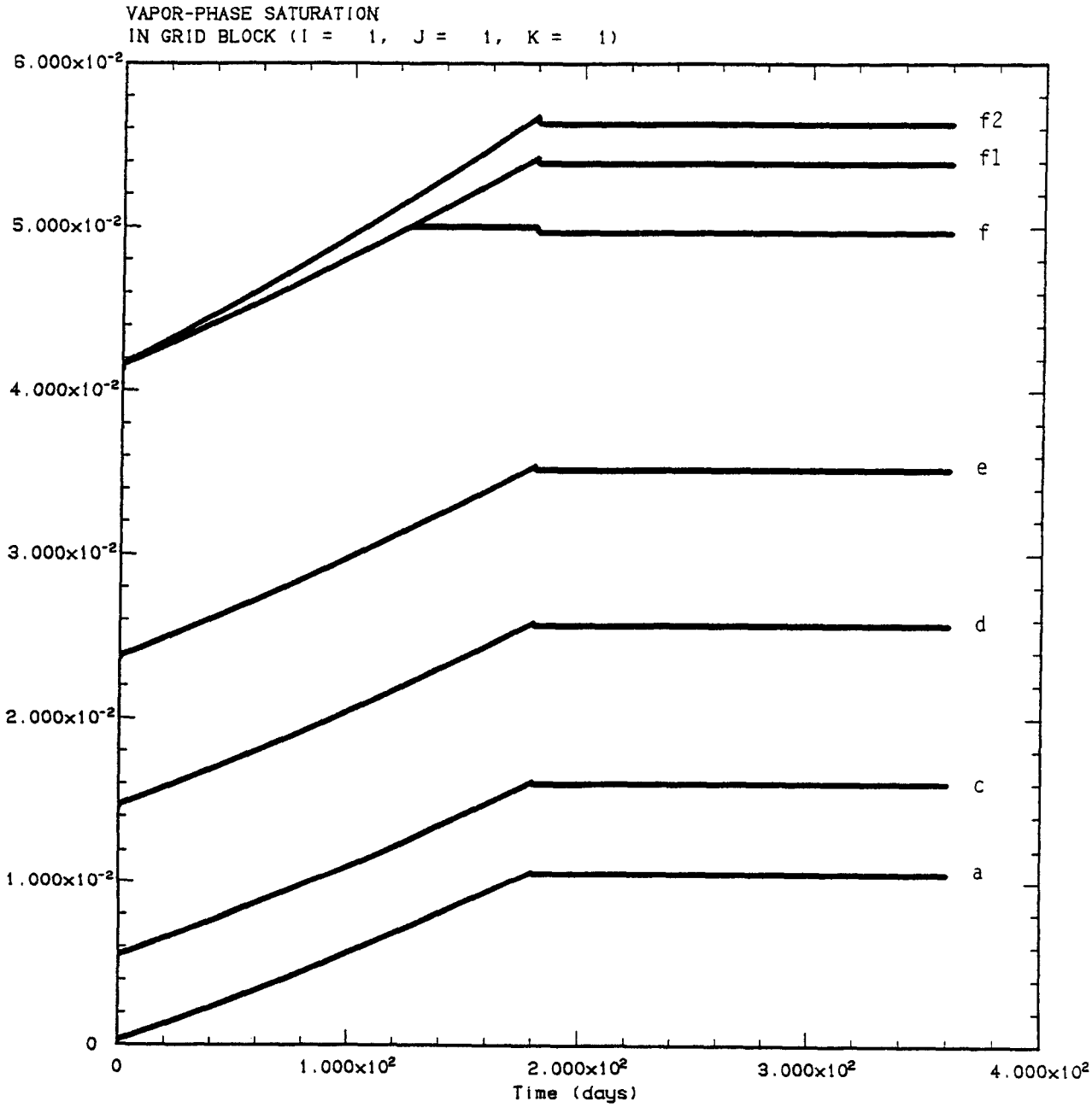

Figure A.1 Effect of gas content on S_g increase near the wellbore when using original Martin R_w and R_g curves (cases a, c, d, e, f) and effect of varying R_w and R_g curves (cases f, f1, f2).

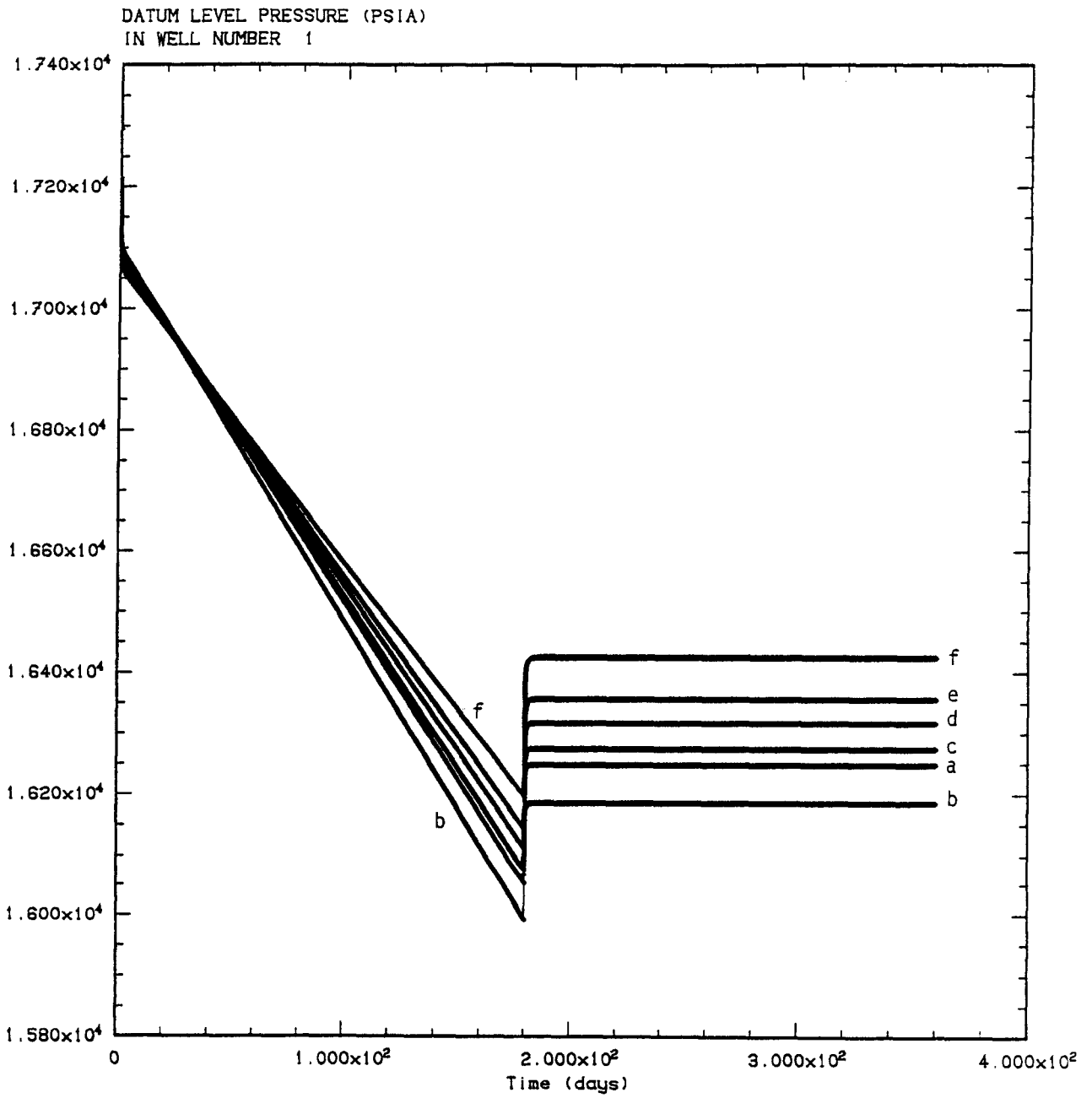

Figure A.2 Effect of gas content on sandface pressure decline rate when using original Martin R_w and R_g curves (cases a, b, c, d, e, f).

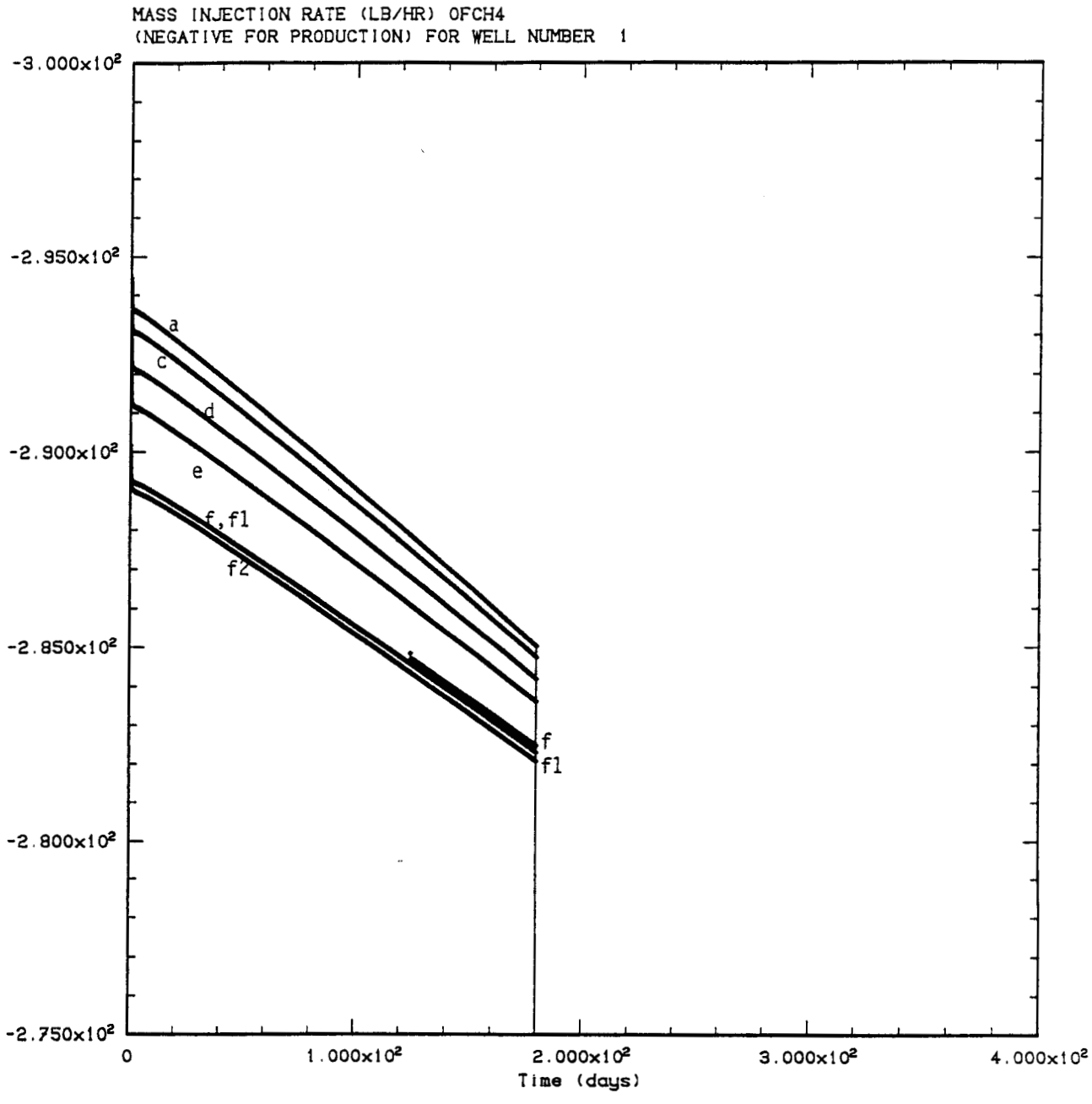

Figure A.3 Effect of gas content on CH_4 production rate when using original Martin R_w and R_g curves (cases a, c, d, e, f) and effect of varying R_w and R_g curves (cases f, f1, f2).

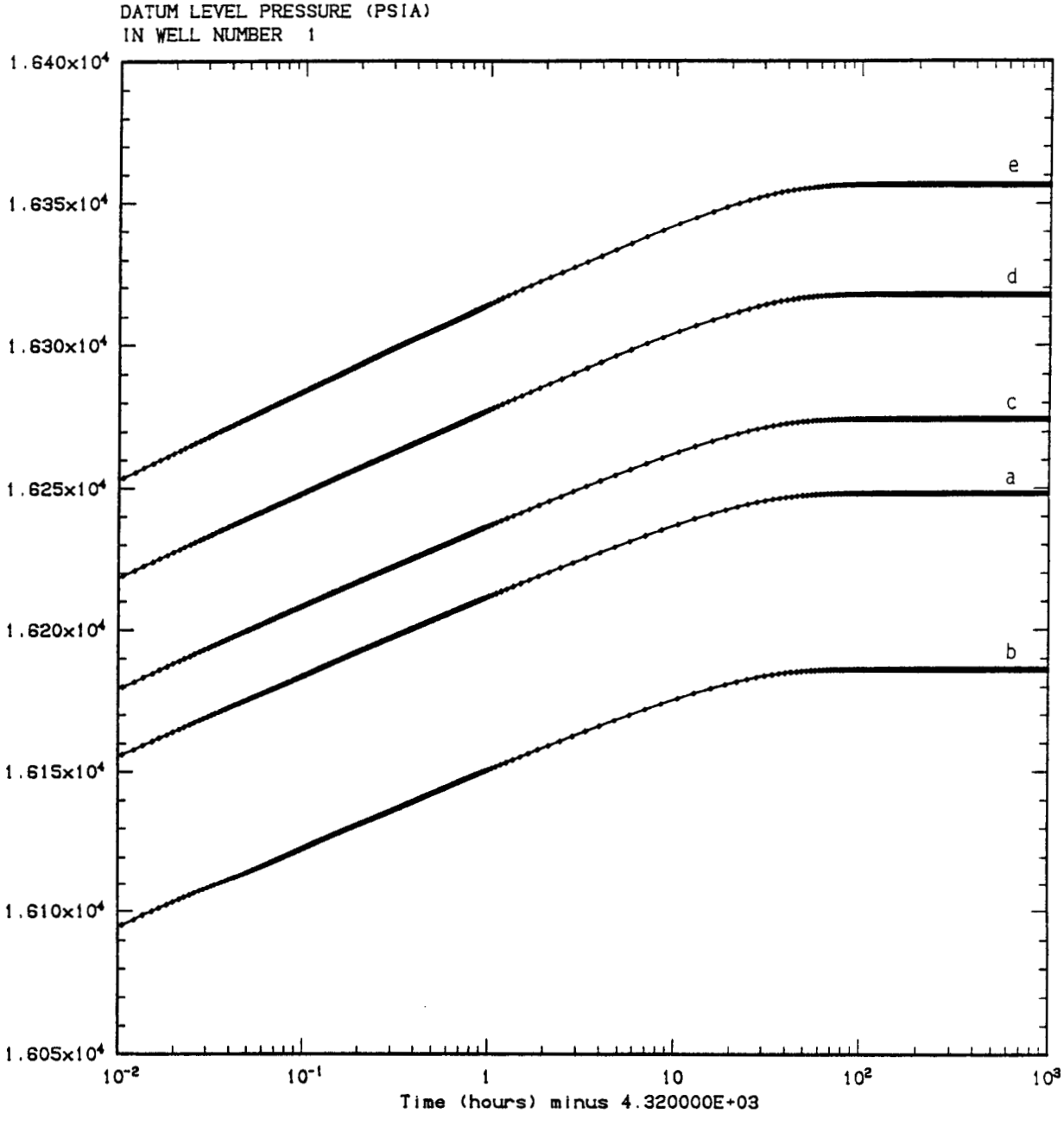

Figure A.4 Effect of gas content on sandface pressure buildup after shutin when using original Martin R_w and R_g curves (cases a, b, c, d, e).

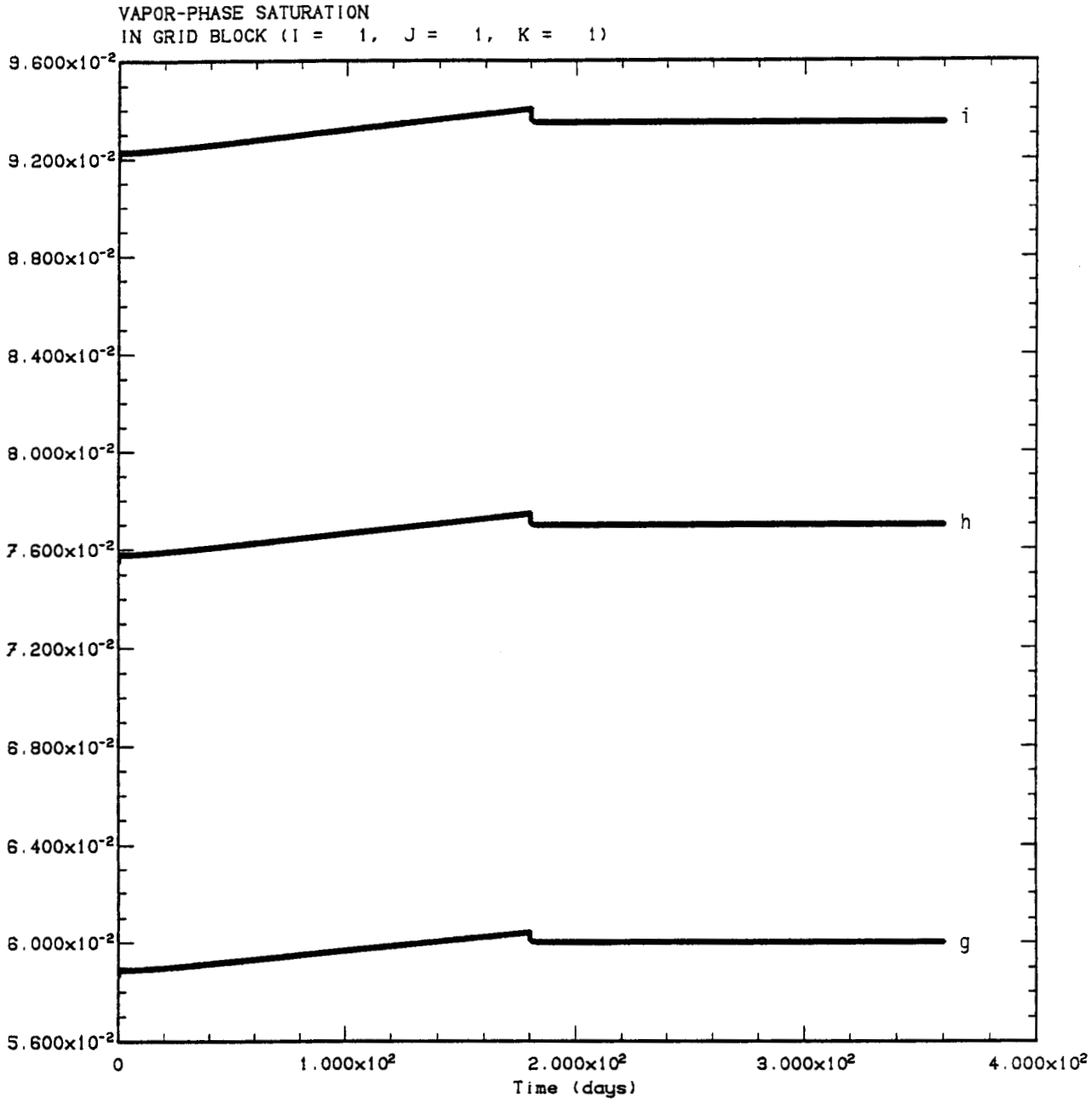

Figure A.5 Effect of gas content on S_g increase near the wellbore when gas phase is mobile from outset of production and when using original Martin R_w and R_g curves (cases g, h, i).

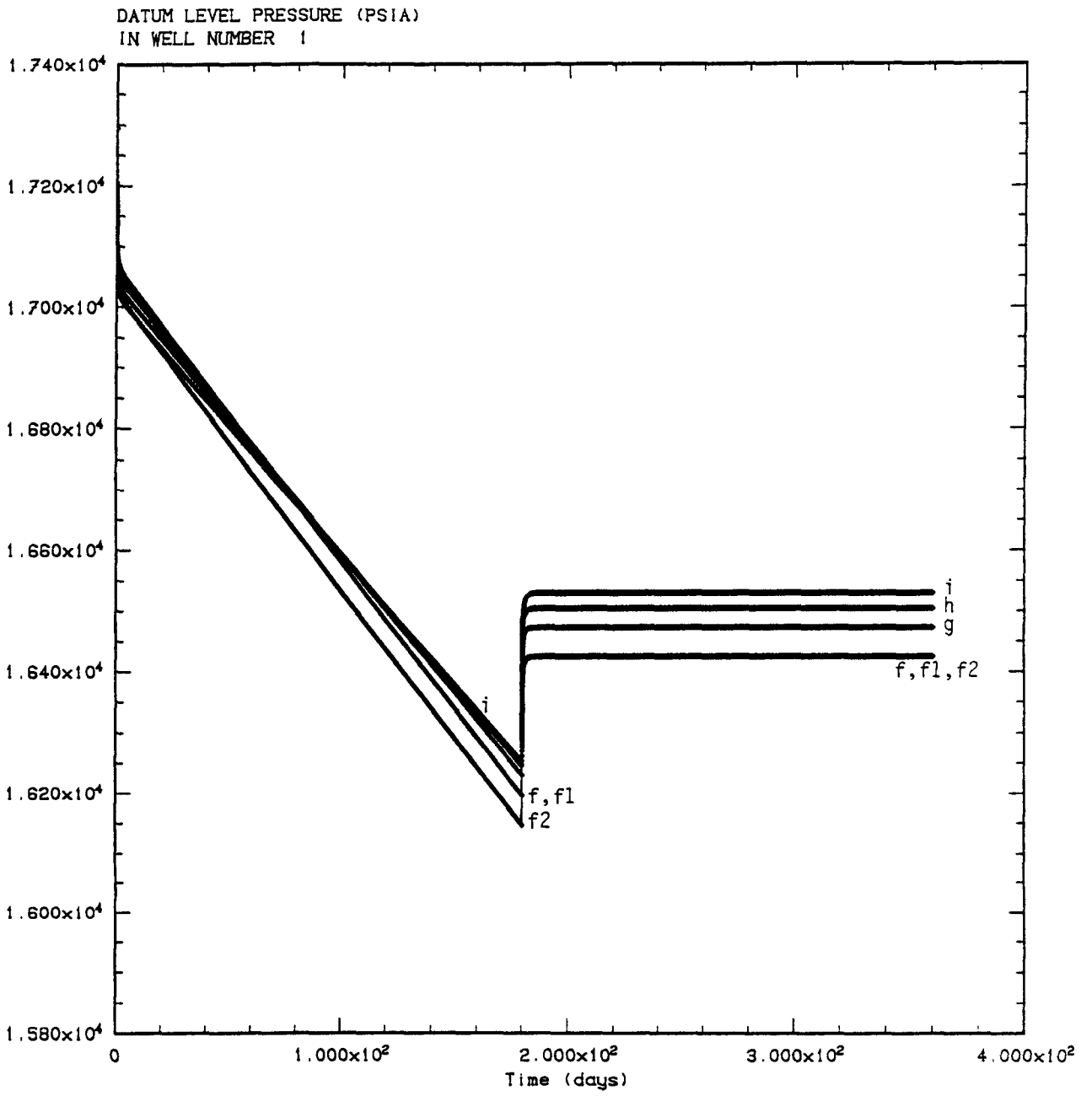

Figure A.6 Effect of gas content on sandface pressure decline rate when using original Martin R_w and R_g curves (cases g, h, i) and effect of varying R_w and R_g curves (cases f, f1, f2).

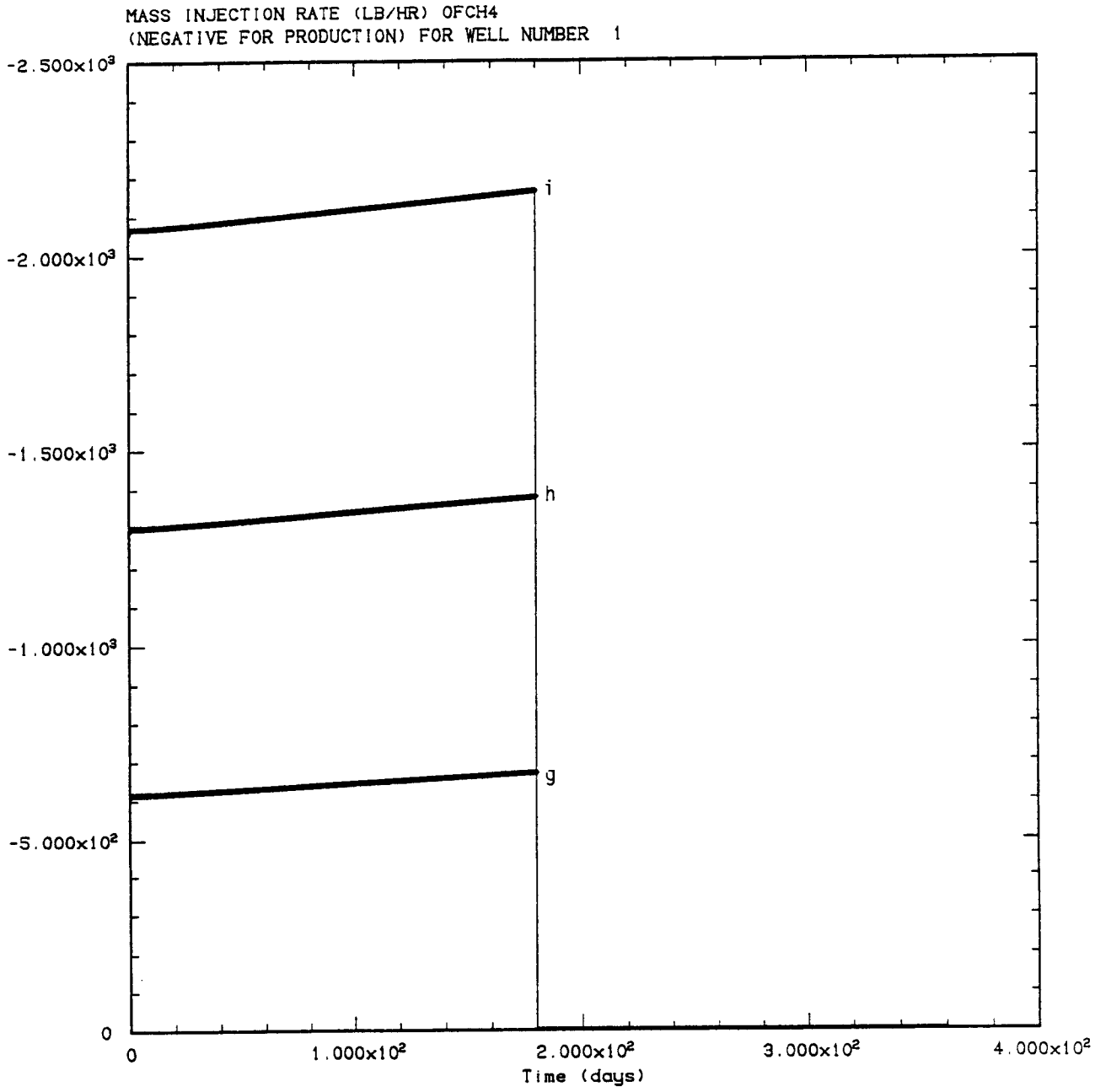

Figure A.7 Effect of gas content on CH_4 production rate when gas phase is mobile from outset of production and when using original Martin R_w and R_g curves (cases g, h, i).

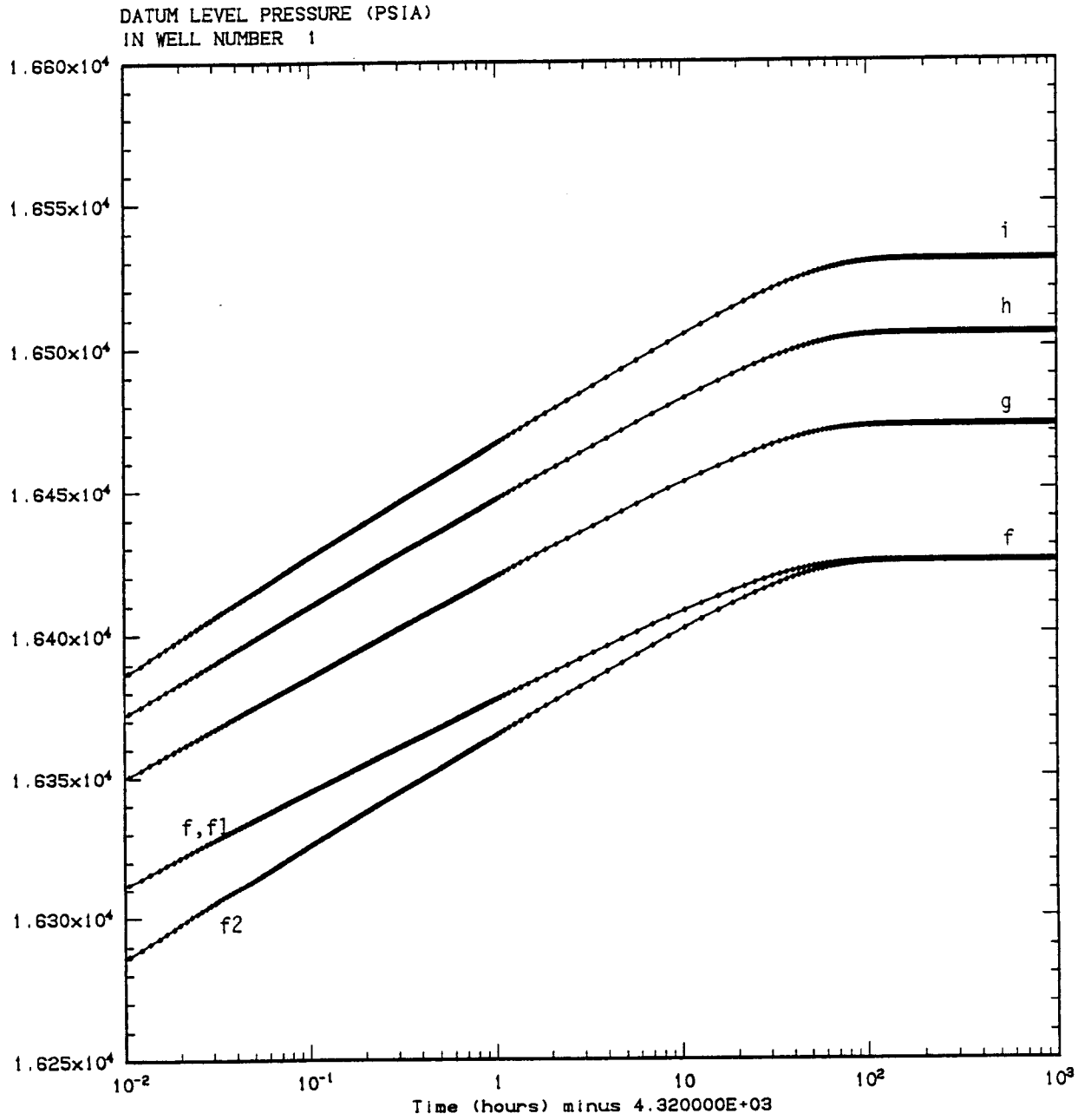

Figure A.8 Effect of gas content on sandface pressure buildup after shutin when using original Martin R_w and R_g curves (cases g, h, i) and effect of varying R_w and R_g curves (cases f, f1, f2).

in Figure A.5. For case i1 there is no free gas produced since the assumed value $S_{gr} = 0.300$ is never attained. Use of the revised Martin R_w curve in case i2 greatly reduces the relative permeability of the liquid phase (Figure 17) causing a more rapid pressure decline than for cases i and i1. The near-well value of S_g in case i2 increases from 0.0920 to $S_{gr} = 0.100$ after ~45 days of production; free gas is produced thereafter. The produced GWR in cases i1 and i2 declines slowly with time (see Table 7). Use of revised Martin R_w curve drastically increases the slope of the pressure buildup curve; the inferred permeability for case i2 is about 36 percent of that that in case b.